UCLouvain

FACULTE DES SCIENCES

**Faculté des sciences**

# Development of a new selection of neutrino events for the IceCube Upgrade

Mémoire présenté en vue de l'obtention du grade académique de Master [60] en sciences physiques

Auteur : Mévisse Guillaume
Promoteur : Prof. Gwenhaël de Wasseige
Lecteurs : Prof. Agni Bethani, Prof. Justin Janquart
École de Physique
Année académique 2024-2025

# Acknowledgement

I would like to express my deepest appreciation to Per Myhr and Karlijn Kruiswijk, with whom I had the opportunity to work, for their always caring help, advice, answers, and invaluable suggestions for this work.
I would also like to thank my supervisor, Gwenhaël de Wasseige, for her dedicated time and expertise.
Finally, I would like to thank my family and friends for their motivation and support during this year.

# AI usage

In this master's thesis, AI tools were used to enhance the overall quality of the work. Specifically, Copilot was employed for code writing, Grammarly for grammar correction and improved phrasing, and ChatGPT for various purposes. Additionally, tools such as Scite.ai and Scispace were used for literature research.

# Contents

# List of Symbols

| Symbol | Definition | Units |
|---|---|---|
| $w$ | Weight of an event | [Hz] |
| $P_{int}$ | Interaction probability for a neutrino event | [-] |
| $S$ | Cross-section used for the simulation | [m²] or [cm²] |
| $\Omega$ | Solid angle | [sr] |
| $\Phi_{\text{phys}}$ | Physical flux of neutrinos | [$\text{cm}^{-2}\text{s}^{-1}$] |
| $\Phi_{\text{phys}}$ | Generated flux of neutrinos in the simulations | [$\text{cm}^{-2}\text{s}^{-1}$] |
| $E$ | Neutrino's energy | [GeV] |
| $N_{\text{flux.ev.}}$ | Number of events in simulated flux | [-] |
| $\epsilon_{\text{LC}}$ | LC efficiency, fraction of physics hits that are categorized as LC | [-] |
| $\Delta t_{\text{PMTs}}$ | Time window between 2 hits on PMTs in the same DOM | [s] |
| $\Delta t_{\text{DOMs}}$ | Time window between 2 hits on PMTs in different DOMs | [s] |
| $n$ or LC span | Number of neighbors up and down used for the LC condition | [-] |
| $\epsilon_{\geq x\%\ \text{hits}}$ | Minimum Hit Fraction Efficiency, fraction of neutrinos for which at least $x\%$ of the physics hits are categorized as LC | [-] |

# Introduction

Neutrinos are light elementary particles that can come from various cosmic sources, such as the Sun (Haxton et al., 2013), active galactic nuclei, or gamma-ray bursts (Mészáros, 2017). They are therefore essential to study the energetic phenomena that occur in the Universe. Moreover, the neutrinos are part of the Standard Model of particle physics and are probably one of its least-known elements. In particular, their mass and oscillation are not well known. They can be a part of evidence toward Beyond the Standard Model physics. Due to their weak interactions and neutral charge, they can traverse large distances without interacting at all, making them very hard to detect, observe, and study.

Neutrinos were observed first in 1956, and this observation was quickly followed, in 1965, by the discovery of atmospheric neutrinos (Reines et al., 1965). Three years later, the Homestake experiment allowed for the first observation of solar neutrinos (Cleveland et al., 1998), which gave the Nobel Prize to Raymond Davis. Since then, neutrino astronomy has grown as a branch of astronomy, providing new insights into the processes in the universe. More generally, this astronomy is part of the continuously developing multimessenger astronomy. Detecting and studying high-energy neutrinos, especially ones with energies larger than what we can produce on Earth, allows us to confront our models and understanding of the fundamental properties of the neutrinos, and then of particle physics.

In this context of neutrino astronomy, the IceCube Neutrino Observatory was built at Amundsen-Scott South Pole Station. Completed in 2010, it relies on the instrumentalization of a cubic kilometer of Antarctic ice. Since its creation, it has contributed to the detection of high-energy neutrinos, their associations with astrophysical objects, and the mapping of the neutrino sky. It also made significant contributions to neutrino oscillations and Beyond Standard Model physics.

Following these results, the IceCube Collaboration planned the IceCube-Gen2 observatory, with the aim to increase the efficiency of neutrino detections at very high energies. Especially, the IceCube Upgrade, consisting of the deployment of new improved sensors in the core of the current IceCube array, is focused on low-energy neutrinos, in the range of the GeV. This Upgrade, planned for 2025-2026, is the first step and a proof of concept towards IceCube-Gen2.

The first chapter will be a presentation of the history of neutrinos, from the beginning of the idea of their existence to their detection and measurements. It will also present neutrino astronomy, starting from how the first astrophysical neutrinos were observed to their use now, and the discoveries they have allowed to do.

In the second and third chapters, we will present the IceCube facility and the IceCube Upgrade in more detail. These chapters will allow us to have a better understanding of the way neutrinos are detected and reconstructed using Cherenkov radiation and optical modules. Then, we will see how the IceCube Upgrade will increase the efficiency of the detection, using new types of sensors that are more reactive. We will also see that the expected data rate is too large and should be handled using a pre-trigger condition, similar to what is done in IceCube. This will be the objective of this master thesis: to define a pre-trigger condition that allows to keep as much signal as possible, while giving a data rate lower than the threshold.

To be able to define this trigger, the fourth chapter will focus on defining the simulations used for the IceCube Upgrade and the way they work. We will see that the noise rate is about 6 MHz, while the rate for the neutrino hits is a few Hertz. Then, we will analyze these simulations in depth, studying the impact of the type of neutrino, their energy level, and other parameters. We will also see what fraction of hits is coming from the different types of sensors, or the number of hits per neutrino.

In the fifth chapter, multiple ways to define the pre-trigger are proposed. We will imagine and improve a new condition to reach a very high fraction of physics hits retained while keeping the rate low enough. Multiple parameters are defined that affect how it works. The next and last chapter will then be a thorough analysis of the results, using parameters leading to the best results. In this chapter, we will see how many neutrinos are detected depending on the properties such as the type of the neutrino or its energy. Finally, using the condition of a rate lower than 3 MHz, we can reach 90 to 95% of hit detection. We will also define another criterion, the Relative Threshold Efficiency, to characterize more efficiently the proposed pre-triggers.

# Chapter 1

# A brief history of neutrinos and neutrino astronomy

The history of neutrinos is a journey through theoretical physics, experimental innovation, and astronomical discoveries. From being a hypothetical particle, they became critical messengers from the Universe and might be the gateway to physics beyond the Standard Model.

Early in the 20th century, physicists encountered a problem: the continuous energy spectrum of emitted electrons in beta decay seemed to violate energy, momentum, and spin conservation. To solve that, in 1930, Wolfgang Pauli hypothesized the existence of a new, neutral particle, around 100 times lighter than the proton. It would later be called the "neutrino", following Chadwick's discovery of the neutron.

In the late 1930s, the first indirect signs of neutrinos appeared: cloud chamber experiments showed unexpected results consistent with Pauli's hypothesis. Due to their very weak interactions with matter, the direct detection of neutrinos would however still have to wait.

In 1956 came the first confirmed detection of neutrinos, through the work of Cowan et al. (1956). They used a nuclear reactor as a neutrino source and observed inverse beta decay interactions in a liquid scintillator detector. In 1962, the existence of the muon neutrino, distinct from the electron neutrino, is demonstrated by Danby et al. (1962). Their experiment proves that neutrinos come in "flavors", which will be essential later.

In 1965, the first detection of a natural neutrino occurred in a gold mine in South Africa (Reines et al., 1965), deep underground and shielded from cosmic rays. Later, in 1975, the tau lepton discovery at SLAC (Perl et al., 1975) hinted at the existence of a third neutrino flavor, the tau neutrino. However, it was discovered only 25 years later, in the year 2000. The DONUT (Direct Observation of the Nu Tau) experiment at Fermilab observed interactions of tau neutrinos (Kodama et al., 2001).

In the 1960s, the Homestake experiment (Cleveland et al., 1998) started one of the most significant mysteries in neutrino physics: the detector, designed to observe solar neutrinos, only detected a third of the number predicted by the models of the Sun. This was solved by the theory of neutrino oscillations (Balantekin and Haxton, 2013), where neutrinos change flavor as they propagate. This idea however implies that neutrinos must have a mass, contradicting assumptions in the Stand Model. This oscillation phenomenon was later validated by the Super-Kamiokande experiment (Fukuda et al., 1998).

In 1987, a supernova, called SN1987A, exploded in the Large Magellanic Cloud, 168000 light-years away from us. This is the first and only time a burst of neutrinos coming from a supernova was recorded, by the Kamiokande II experiment in Japan: 12 neutrinos are detected over 13 seconds. This was sufficient to confirm theoretical models that most of the supernova's energy is released by neutrinos (Hirata et al., 1987). It also marked the birth of neutrino astronomy.

In recent decades, neutrino astronomy has become an essential tool in exploring the Universe's phenomena. In this context, the IceCube Neutrino Observatory represents a leap forward in detecting high-energy neutrinos, having already identified multiple neutrinos with energies exceeding 1 PeV, far beyond the energy of neutrinos produced in our accelerators. We will describe some of these discoveries later.

Last year, the deep-sea KM3NeT detector, in the Mediterranean Sea, announced the detection of an ultra-high-energy neutrino event (about 120 PeV) (Aiello et al., 2025). This is the most energetic neutrino detected to date, and it might be the first detection of a cosmogenic neutrino, or come from a different cosmic accelerator than the lower-energy neutrinos already detected. This reinforces the role of neutrinos as probes to the most extreme events in the Universe.

We have seen how neutrinos, from a theoretical fix, have become a major particle in understanding both particle physics and astrophysics. From this overview, we will now develop the context of this work: the IceCube Neutrino Observatory.

# Chapter 2

# The IceCube Neutrino Observatory

The IceCube Neutrino Observatory is a research facility designed to detect high-energy neutrinos from astrophysical sources. It detects neutrinos using their interaction with ice. It is located in Antarctica, at the Amundsen–Scott South Pole Station, where the deep and old ice has excellent optical properties. Finished in December 2010, the volume of IceCube is one cubic kilometer, making it the world's largest neutrino detector (Abbasi et al., 2009). In this chapter, we will describe the observatory, how it works, and the interactions used to detect neutrinos. Then, we will see how the data are treated in the IceCube, only describing the parts that will be useful for this work.

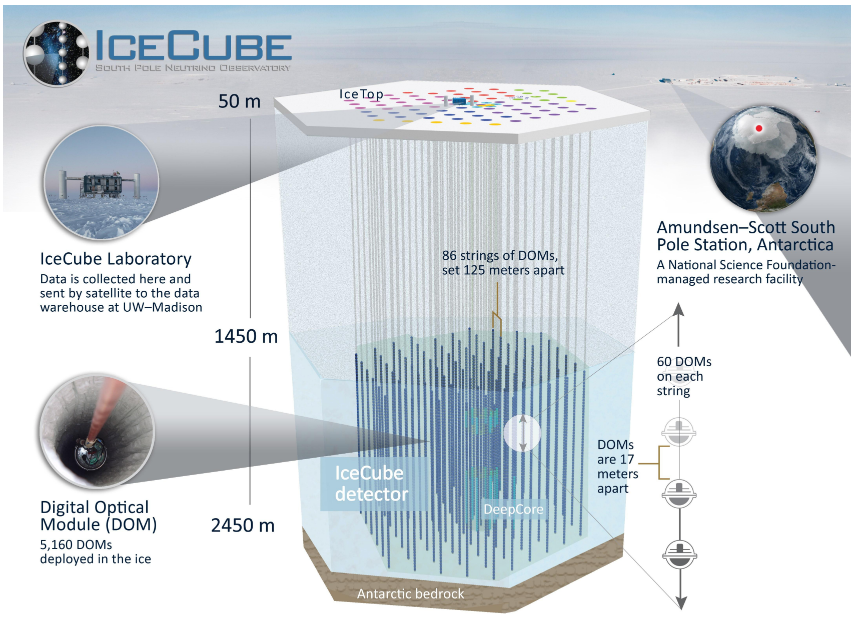


Figure 2.1: The Icecube detector (ice, 2025)

## 2.1 Description of the facility

The observatory is composed of 5,160 Digital Optical Modules that we will call DOMs, each equipped with a photomultiplier tube (PMT) and onboard digitization electronics. These DOMs are deployed along 86 vertical cables between 1,450 and 2,450 meters below the surface of the ice. The cables allow for the mechanical support of the DOMs, and their electrical and data connectivity. This configuration allows for a 3D dense distribution of the sensors, which makes it possible to track the energy and direction of detected neutrinos. This depth also ensures minimal contamination from atmospheric muons.

IceCube detects Cherenkov radiation flashes of blue light emitted when secondary charged particles, produced by neutrino interactions, traverse the ice faster than light travels in that medium, as illustrated in Figure 2.2. The PMTs capture this light and express it as an electric signal, a pulse. Collecting the signals from multiple PMTs allows for the reconstruction of the energy and direction of the neutrino.

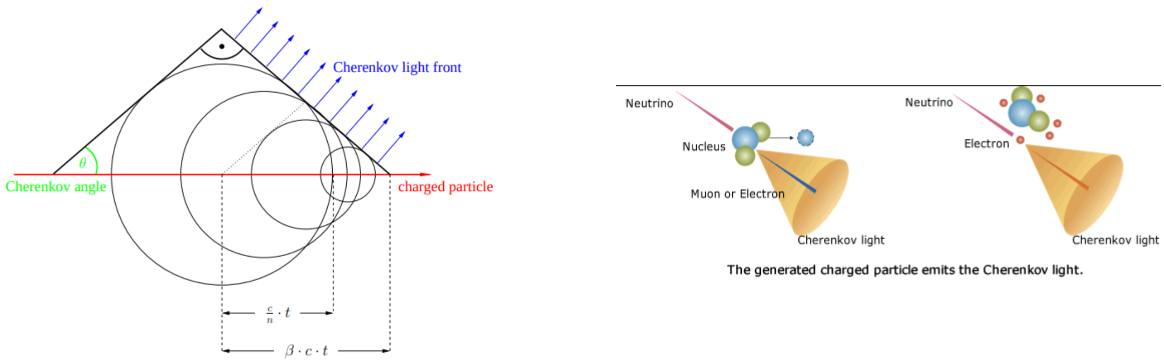


Figure 2.2: Illustration of the Cherenkov radiation and its detection by a PMT (Gluesenkamp, 2010).

The IceCube Neutrino Observatory offers one specific and distinctive feature: its location within the Antarctic, and its use of a very large volume of ice. This offers advantages compared to classical water-based detectors. The optical properties of deep ice provide a clear medium for detecting the Cherenkov radiation. In contrast, water-based detectors benefit from better angular resolution because of the large scattering length in water, but the water leads to more noise coming from bioluminescence, and radioactive decay of particles such as potassium-40, therefore requiring a more complex algorithm for the filtering. Furthermore, ice is a stable and inert medium, whereas water detectors must contend with mechanical challenges posed by currents and marine biofouling. While both media offer complementary advantages, the clarity and stability of Antarctic ice make it particularly well-suited for large-volume, long-term neutrino detection (Spiering, 2020).

## 2.2 Neutrino events

Neutrinos are very elusive particles: they are electrically neutral and interact only via the weak nuclear force. It makes them capable of passing through large distances of solid matter without interacting. Therefore, their detection requires large and very sensitive volumes.

IceCube detects neutrinos indirectly, by observing the secondary charged particles they produce when they interact with the nuclei of atoms in the Antarctic ice. These interactions are rare, but when they happen, they can produce particles like muons, electrons, or taus.

There are two types of interactions: neutral current (NC) and charged current (CC). The neutral current interaction relies on the exchange of a Z boson with a nucleon in ice (here called $N$). The neutrino transfers part of its energy to the nucleon, which generates a hadronic shower of particles ($X$) ($l$ indicates the flavor of the neutrino) :

$$\nu_l + N \longrightarrow \nu_l + X$$

For the charged current interaction, the neutrino exchanges a W boson with a nucleus in ice. This generates a lepton corresponding to the flavor of the neutrino, and a hadronic shower similar to the neutral current interaction :

$$\nu_l + N \longrightarrow l^- + X$$

The charged particles (leptons or hadronic showers) then travel through the ice at speeds faster than light can move through the same medium. This superluminal travel emits a faint blue glow called Cherenkov radiation (Yuan, 2023), an optical version of a sonic boom.

Then, the photons from the Cherenkov radiation interact with the PMTs, generating a pulse. The data from all the pulses allows the reconstruction of the neutrino properties such as energy and direction. Depending on the neutrino type and interaction, there are multiple topologies of possible events, illustrated in Figure 2.3. These depend on the interaction of the neutrinos with the nuclei in ice.

- Track events: light deposited symmetrically around the particle trajectory, caused by a particle going in a straight line, triggering the PMTs. This is only the case with muon neutrinos. The direction of these neutrinos is therefore easy to reconstruct.
- Cascade events: for electron and tau neutrinos, the charged and neutral current interactions can lead to a cascade-like event, with a spherical but non-isotropic shape. It is therefore harder to reconstruct their direction.
- Double-bang events: for high-energy tau neutrinos, a "double bang" event is theoretically expected, because of the creation of a tau lepton with a cascade (first bang). Then, the tau lepton disintegrates in a second cascade, generating the second bang. However, these events still have not been detected clearly (Fargion et al., 2016), but 7 tau candidates have been detected recently (Abbasi et al., 2024).

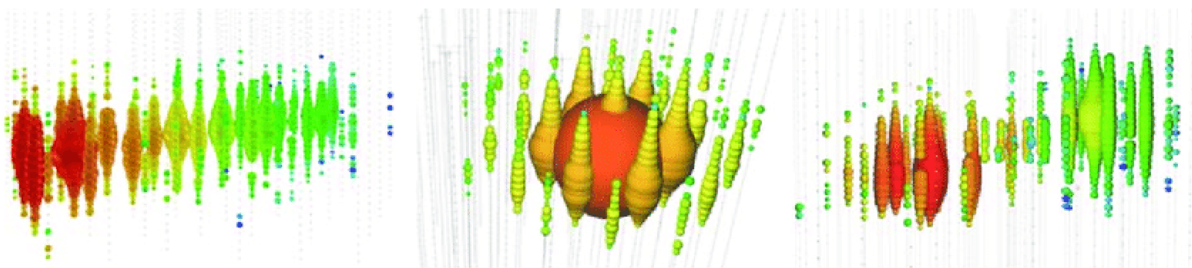

Figure 2.3: Typical event signatures observed by IceCube: a track-like event (left), a showerlike event (middle), and a double-bang event (right). Each colored sphere marks a DOM that records Cherenkov's light. The first and second are events observed by IceCube while the third is a simulation. Colors indicate the relative time of the photons concerning each other (early photons are red, and late photons are blue). The size of the dot corresponds to the number of photons (Kowalski, 2017).

## 2.3 Hits processing in IceCube

When a photon interacts with a PMT, it is converted into a detectable increase in voltage by accelerating electrons through a photocathode. This signal is then amplified and, if exceeding a threshold of 25% of the voltage generated by a single photon, it is digitized and timestamped with nanosecond accuracy (Abbasi et al., 2009). This is called a "physics hit" and will be the basis for our later work. The term "hit" will more generally include signals from noise, background, etc.

IceCube relies on satellite connection to transfer its data, limiting data export. Therefore, it is necessary to reduce the noise and only keep the interesting hits. From now on, we will call physics hits all the hits that come from a neutrino and are therefore not noise. The first filtering is done using the Local Coincidence (LC) pre-trigger. The first type is the Hard Local Coincidence (HLC) illustrated in Figure 2.4, which can happen in 2 cases: if two neighboring DOMs have a hit within a time window of 1 µs (LC1) or if two hits are found within the same time windows, but checking the two upper and lower neighbors (LC2). In the case of an HLC, the full hit is digitized. The second type is the Soft Local Coincidence (SLC), less used, and is active even if there are no neighboring DOMs with a hit. In this case, less information is digitized (Aartsen et al., 2017). For the remainder of this work, it is useful to note that this Local Coincidence is applied using hardware: cables connect neighboring DOMs, meaning that the LC pre-trigger is applied without the need for a computer.

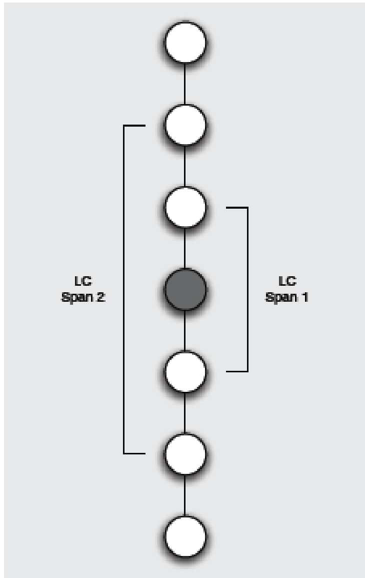

Figure 2.4: Illustration of the Hard Local Coincidence trigger.

Figure 2.5 shows the difference in hits for an event, using only the HLC condition and the SLC condition. The HLC gives a much clearer picture of the event, and therefore a much simpler analysis. However, the SLC condition can be very useful, for example, in the FPT (Faint Particle Trigger), which is specifically designed to detect rare, low-signals particles such as fractionally charged particles (Stuerwald, 2024).

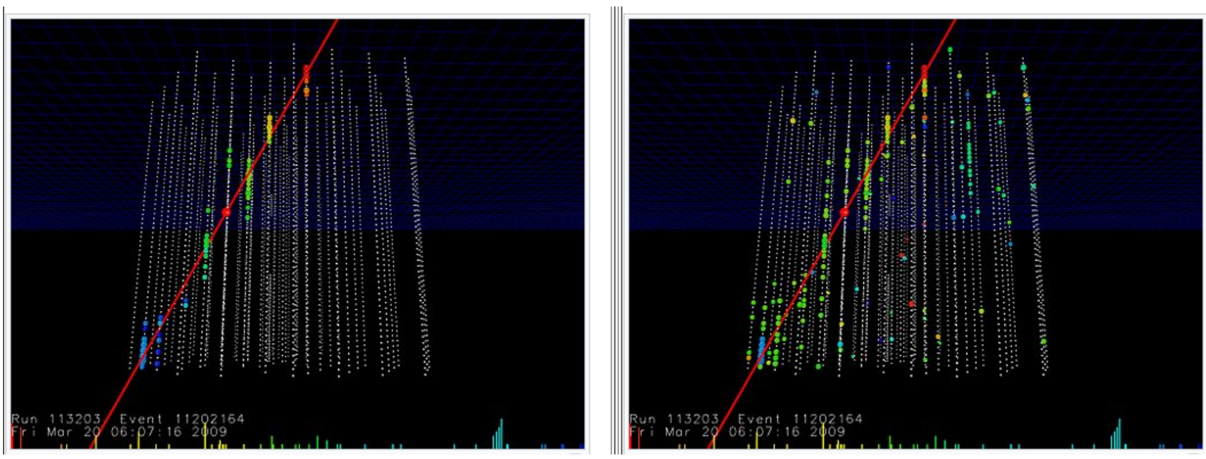

Figure 2.5: Comparison of the same events with the HLC only (on the left) and with both HLC and SLC (on the right).

After this, there are a few more steps of filtering and triggering. The data is then compressed and transferred using a specialized data format using a framework called "IceTray". This system allows the people from the collaboration to get all the detailed information from the events, such as the timing, location of DOMs, etc., which is needed for the post-treatment and analysis of the data. We will not detail all these steps in this description, as the work presented here will only focus on the Local Coincidence condition.

## 2.4 Some results from the collaboration

Since its completion in 2010, the IceCube Neutrino Observatory has delivered groundbreaking results across multiple domains of astroparticle physics. Designed to detect high-energy neutrinos from cosmic sources, IceCube has provided the first strong evidence for the existence of an astrophysical neutrino flux, contributed to multi-messenger astronomy, and placed new constraints on fundamental physics.

One of IceCube's steps was the first detection of high-energy neutrinos of extraterrestrial origin, in 2013. These neutrinos, with energies exceeding 60 TeV and even reaching PeV, can not be explained by atmospheric backgrounds. This discovery marked the beginning of neutrino astronomy (IceCube, 2013).

In 2017, IceCube detected a high-energy muon neutrino (IceCube-170922A) and sent out a real-time alert. Follow-up observations across the electromagnetic spectrum—gamma rays, X-rays, and radio—led to the identification of the blazar TXS 0506+056 as a likely source. This was the first compelling association between a neutrino and a known astrophysical object and proof of the use of neutrinos in multimessenger astronomy (Aartsen, 2018).

In 2023, the IceCube Collaboration published the first full-sky map of high-energy neutrino emission, revealing an excess of neutrinos from the Galactic plane, particularly from the central regions of the Milky Way. This result confirmed that our galaxy contributes to the diffuse astrophysical neutrino flux at about  10% (Abbasi et al., 2023b).

We have highlighted that the IceCube facility has provided groundbreaking results in astrophysics and neutrino physics. These results prompted work on an upgrade of the IceCube observatory, simply called the IceCube Upgrade, which will be described in more detail in the next chapter.

# Chapter 3

# The Icecube Upgrade

Following the results of the IceCube facility, a project called PINGU (Precision IceCube Next Generation Upgrade) was proposed (Aartsen et al., 2014). The project was however changed to the smaller IceCube Upgrade, launched in 2019. It aims to significantly improve the sensitivity to low-energy neutrinos, refine its calibration capabilities, and lay the technological groundwork for the future IceCube-Gen2 observatory (Aartsen et al., 2021). The deployment of the upgrade is expected during the 2025–2026 austral summer. In this chapter, a presentation of the upgrade will be given.

## 3.1 Objectives of the Upgrade

IceCube was originally optimized and designed to detect high-energy neutrinos from astrophysical sources, especially in the TeV to PeV range. However, neutrinos from astrophysical sources exist at lower energies, from a few GeV to hundreds of GeV. Of course, these are also scientifically rich. In this range, they are crucial for studying atmospheric neutrino oscillations, which can shed light on the neutrino mass ordering and help test physics beyond the Standard Model, such as sterile neutrinos and non-standard interactions.

This upgrade will significantly improve the ability to reconstruct low-energy neutrino events. This is key for detailed studies of neutrino oscillations, which are sensitive to the mass hierarchy, an open question in particle physics (Ma, 2020). Additionally, precise calibration of the Antarctic ice will reduce one of the major sources of systematic uncertainty in the current detector. The new calibration can be applied retroactively to past IceCube data, providing an instant improvement in all results.

Furthermore, the IceCube Upgrade is a testbed for future technologies that will be deployed in IceCube-Gen2, a much larger array planned to increase the instrumented volume to eight cubic kilometers. Gen2 aims to enhance both the astrophysical reach of the detector and its ability to probe new physics.

## 3.2 Technical details

To fulfill the scientific goals of the IceCube Upgrade, seven new strings will be deployed in the core of the existing IceCube array, equipped with densely packed optical sensors. Approximately 700 optical modules will be installed at depths ranging from 2,150m to 2,450m in the ice. Three designs of sensors will be used: the multi-PMT Digital Optical Module (mDOM), the Dual optical sensor in an Ellipsoid Glass (DEgg), and the Precision

Digital Optical Module (PDOM) (Nagai and Ishihara, 2019). They are designed to improve the photon collection efficiency, improve the angular acceptance, and enhance the accuracy of time and charge measurements, particularly for neutrinos with energy from 1 to 100 GeV (Abbasi et al., 2021). The new strings are illustrated in Figure 3.1.

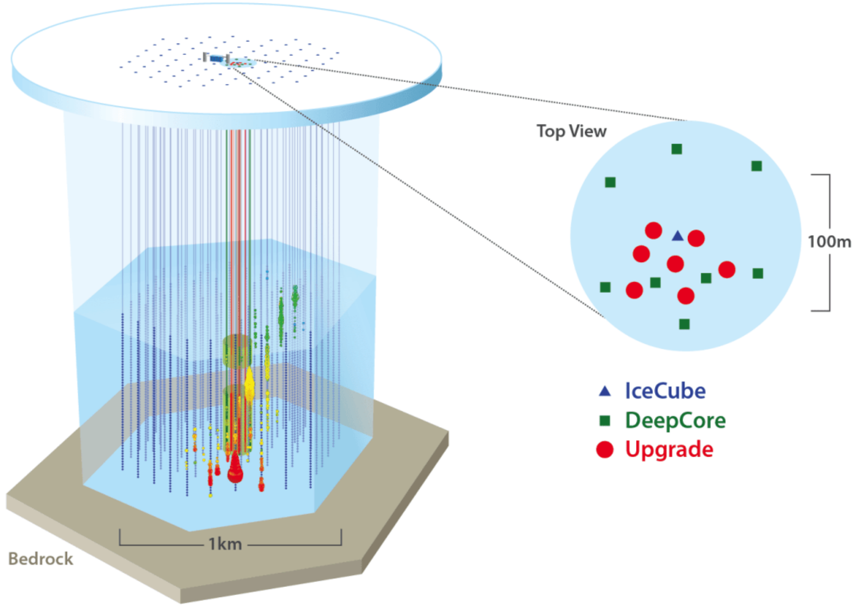


Figure 3.1: Illustration of the Upgrade. The IceCube Upgrade strings will be placed deep within the core of IceCube.

The mDOM is a spherical optical module with a diameter of 36 cm, with 24 photomultiplier tubes of a diameter of 76 mm. These PMTs are distributed uniformly to cover the entire solid angle. This configuration allows precise reconstruction of the directionality of the Cherenkov light emitted. Each PMT is independently digitized with a temporal resolution of less than 1 ns, using electronics capable of sampling up to 960 million samples per second. The total effective area is approximately $0.2\text{m}^2$, significantly improving sensitivity over the current DOMs.

The DEgg features two 203mm PMTs mounted on opposite faces of an ellipsoidal housing. The total height of the module is 38 cm, and the width is about 30 cm. The up-and-down facing configuration allows efficient detection of both upward-going and downward-going light, improving the reconstruction of particle tracks and showers, especially in low-energy regimes. The DEgg's shape, combined with its use of PMTs with high quantum efficiency, results in a significantly larger photon detection area compared to IceCube's original modules (Nagai and Ishihara, 2019).

The PDOM retains the original IceCube DOM basic geometry (a spherical housing with a 254 mm PMT) but incorporates improved internal electronics for better timing, power management, and communication. Sampling rates and dynamic ranges have been improved, and the updated firmware allows more flexible triggering and readout. These modules serve as a baseline to compare against the performance of the newer mDOMs and DEggs. Their inclusion also ensures compatibility with the existing IceCube hardware, making the integration of future large-scale deployments like IceCube-Gen2 easier (Nagai and Ishihara, 2019).

Together, these upgraded sensors will increase the total effective photocathode area by nearly a factor of four. The strings will also carry dedicated calibration devices, such as isotropic light sources, cameras, and neutron generators. These instruments will allow high-precision measurements of the optical scattering and absorption properties of the ice, down to the meter scale, reducing one of the largest sources of systematic uncertainty in neutrino energy and direction reconstruction. Importantly, these calibration improvements will retroactively benefit existing IceCube data as well.


Figure 3.2: Illustrations of the mDOMs (Abbasi et al., 2021), DEggs (Abbasi et al., 2023a), and PDOMs (Nagai and Ishihara, 2019) used for the IceCube Upgrade.

The seven strings installed will be different from the current IceCube strings. In particular, each string will be connected to a computer at the surface, called a StringHub. This is where the LC condition will be applied, and then the data will be sent to computers applying higher-level filters.

Finally, the Upgrade will be made of three regions: the upper layer (from 0 to 2000m deep) will have mainly calibration devices. Then, ranging from 2150 to 2450m deep approximately, the "physics region" will be the place where most of the mDOMs and DEggs are placed. Finally, the deepest part will be another calibration region, deeper than the current IceCube. This will be the first time that we can study this deeper ice (Ma, 2020).

## 3.3 Expected rate and need for a filtering

As we will see in the next chapter, the new sensors in the IceCube Upgrade lead to a much larger expected rate of pulses, about 6 to 7 MHz. However, the hardware limits the rate to about 3 MHz. There is therefore a need for an update of the Local Coincidence trigger, adapted to the upgraded components. The noise dominates the total rate by a factor of a million, as we will see in more detail in the next chapters, which means that we should be able to suppress most of the noise while keeping the physics hits.

The objective of this work is now clear: we need to find a Local Coincidence trigger and its parameters to set the rate at least lower than 3 MHz, while keeping as many physics hits as possible. Once we find suitable parameters, an in-depth study of the behavior of the LC condition will be carried out to determine what set of parameters is best suited for the Upgrade, and what other sets could be used if the conditions of the Upgrade were to change.

# Chapter 4

# Analysizing the simulations

The calibration of the IceCube Upgrade relies on Monte Carlo simulations, modeling both the neutrino interactions and the detector response in ice. In this chapter, the aim is to describe the simulation tools, how they are used, and to have a look at the results obtained from them. The simulations will be analyzed as a first step toward creating an optimal filtering system for the upgrade.

It is essential to note that, from here, we will only consider the IceCube Upgrade: we will take the seven strings as separated from the current IceCube array, meaning that the rates and events are studied only on these seven strings. Therefore, some events will be incomplete, as the neutrinos also interact with the current IceCube, but these parts are not important to us: our aim is to limit the hit rate in the IceCube Upgrade to a threshold value, in this case, 3 MHz, while losing as little information as possible.

## 4.1 Description of the simulations

In IceCube, the Monte Carlo simulations of neutrino events consist of multiple steps. The first stage involves simulating neutrino interactions in and around the detector using tools like GENIE (Generates Events for Neutrino Interaction Experiments) (Andreopoulos et al., 2010) for low-energy neutrinos and NuGen (Neutrino Generator) for higher-energy events. These frameworks model neutrino cross-sections with matter and the production of secondary particles such as electrons, muons, taus, and hadronic particles.

Once secondary particles are generated, the Cherenkov light emission is simulated. Modeling how this light propagates through the ice is a critical challenge because the Antarctic ice is not perfectly uniform, leading to variations in its scattering and absorption properties. To model this, a photon propagation tool called CLSim was developed, which is a GPU-accelerated program that simulates how individual photons scatter and are absorbed as they travel through the ice (Schwanekamp et al., 2022). It should be noted that for now, the simulations for the IceCube Upgrade don't include the properties of the holes drilled in the ice, which could affect the simulations.

Simulated photons that reach a sensor are then processed through detector response simulations, which account for quantum efficiency and angular acceptance of the PMTs (especially for new mDOMs and D-Eggs), electronics response, digitization, and data acquisition triggering. At this step, the noise is generated, using a software developed by the IceCube collaboration, Vuvuzela. It models the radioactive background, the scintillation, etc., in the IceCube Upgrade array. This step is probably the one that is the least precise: it is hard to estimate noise, and it is done using currently available noise data from the existing IceCube array and upgrade sensors. These steps are illustrated in Figure 4.1.

The last step consists of the reconstruction and analysis of the simulated events for validation. This step uses reconstruction algorithms, machine-learning methods, etc., and will not be described further here, as the work is focused on filtering the data obtained from the previous step.

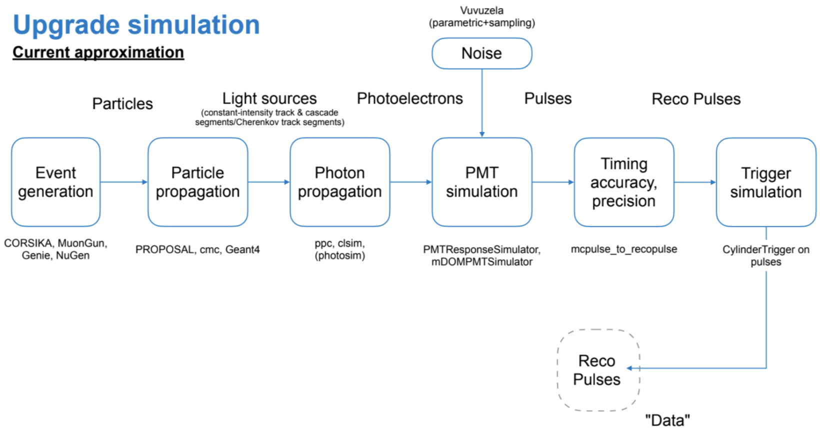


Figure 4.1: Illustration of the simulation workflow. The step we will be working on is the "trigger simulation".

## 4.2 Pulses data

For the Local Coincidence filtering, we need only basic information from each hit. Especially, as we are filtering in-situ, only using the hardware and simple rules. The useful information is therefore the time of the hit, the location of the sensor, and its type -mDOM, PDOM, or DEgg-. Finally, we also need to know if the simulated hit comes from the noise or from a neutrino.

The data are structured in frames. For the non-noise simulations, each frame is associated with one neutrino with a defined energy, ranging from 1 to 500 GeV. For the rate computation, the frame is weighted, and this will be explained in Section 4.3. In each frame, we have multiple hits linked to the PMT from which it originates. There are six types of files, one for each neutrino type: electron, tau, and muon neutrinos and antineutrinos. They therefore contain fewer hits, part of them are physics hits generated by the neutrino, and part of them is noise from different sources. In Figure 4.2, we see the fraction of the total physics hits depending on the energy level of the electron neutrino. The profile is similar for all the neutrino types (For now, we will only use the electron neutrinos for illustration purposes). As we can see, half of the hits come from very low-energy (less than 20 GeV) neutrinos. This is however without the weighting, as we will see now.

We also have noise files, which simulate the noise coming from all sources. They are generated for a duration of 1 second each, making them easy to weight, as the number of hits in the file is the exact expected noise rate. As we will see, this rate is much larger than the expected rates for neutrinos.

## 4.3 Weighting and rate computation

In Monte Carlo simulations of neutrinos, such as those generated with the GENIE software, not every simulated event directly represents an absolute physical probability.

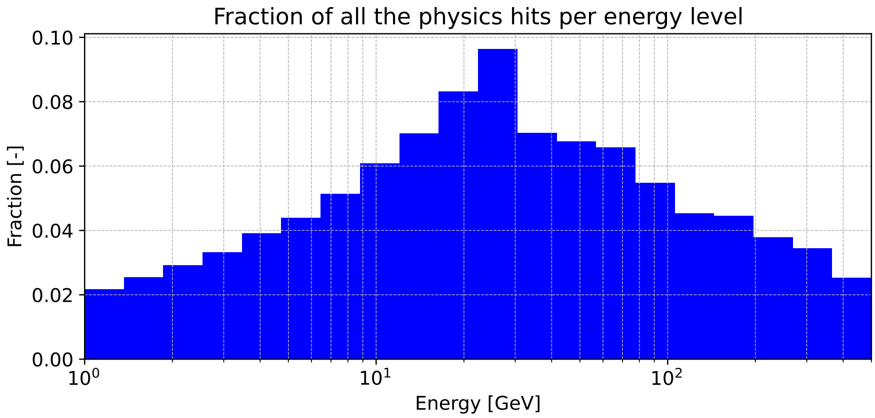


Figure 4.2: The spectrum of physics hits and energy level, using a logarithmic scale. We see most of the hits come from low-energy neutrinos. The peak at the center is due to the logarithmic scale used. However, the hits here are not weighted, which means they don't take into account the expected rates of the neutrino events.

Indeed, in order to generate enough statistically significant events in all relevant phase regions (especially those with low probability), generators like GENIE produce events artificially, with artificial spectra and geometries. Consequently, a weighting factor is applied to each event to correct the event distributions from the generation process and obtain physically interpretable results.

The weight of an event, often noted as $w$, is calculated to represent the actual probability of occurrence of this event under the experimental conditions targeted. It depends on several factors: the neutrino flux model used, the effective cross-section of the interaction, the volume and density of the target, and the generation conditions imposed during simulation. For the IceCube simulations, it is formally written as :

$$w = P_{\text{int}} \cdot S \cdot \Omega \cdot \frac{\Phi_{\text{phys}}(E, [\theta, ...])}{\Phi_{\text{gen}}(E)}$$

where $P_{int}$ is interaction probability, $S$ is the cross-section of the generated cylinder, $\Omega$ is a solid angle in which the neutrinos are generated,$\Phi_{phys}(E, [\theta, ...])$ is the physical flux which can depend on the energy, the angles, etc. and $\Phi_{gen}(E)$ is the generated flux.

For the files used here, the generated spectrum follows a power law with $\gamma$ and $A$ parameters :

$$\Phi_{\text{gen}}(E) = AE^{-\gamma}$$

We also have the number of flux events $N_{flux.ev.}$ which is the number of events in the simulated flux (before interacting with the sensors). Using

$$N_{\text{flux.ev.}} = A \int_{E_{\min}}^{E_{\max}} E^{-\gamma} dE$$

We get

$$w = P_{\text{int}} \cdot S \cdot \Omega . \frac{\int_{E_{\min}}^{E_{\max}} E^{-\gamma} dE}{N_{\text{flux.ev.}} E^{-\gamma}} \Phi_{\text{phys}}(E, [\theta, ...])$$

In the GENIE simulations, a value is stored for each event, the "$OneWeight$", which is

$$OneWeight = P_{\text{int}} \cdot S \cdot \Omega \cdot \frac{\int_{E_{\min}}^{E_{\max}} E^{-\gamma} dE}{E^{-\gamma}}$$

Therefore, the weight is finally

$$w = \frac{OneWeight}{N_{\text{flux.ev.}}} \Phi_{\text{phys}}(E, [\theta, ...])$$

The physical flux is represented using a power-law spectrum[1] (Aartsen et al., 2015):

$$\Phi_{\text{phys}}(E, [\theta, ...]) = AE^{-\gamma} = 0.02E^{-2.5}$$

The weight of events depending on the energy of the electron neutrino is shown in Figure 4.3. The curve is the same for the other types of neutrinos.

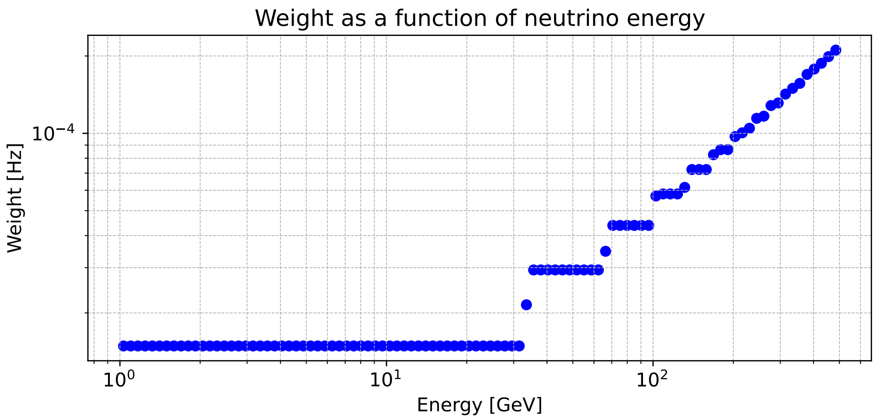


Figure 4.3: Weight as a function of energy for the electron neutrinos, using a logarithmic-logarithmic scale. The increase in energy is linear, with steps of about 30 GeV. The weight is larger for high-energy neutrinos.

In the end, what we mainly need is the expected rate for each interaction and how often the detectors see light from these interactions. This is easily computed as the product of the number of hits for the simulated event times its weight. For the noise files, the simulation has a unitary weight, because the simulated time is one second. We can therefore compute the expected rate for each type of neutrino and the global noise, which is much larger as seen in Figure 4.10. For the rate computations later, we will only consider the noise files, as the neutrinos have negligible rates. It should be noted that the rates computed here are therefore the rate of pulses and not the rate of events.

In Figure 4.5, we see the fraction of physics hits, after being weighted, depending on the energy level. The fraction at low energy is much smaller than in Figure 4.2. Especially, we see that about 55% of the physics hits come from neutrinos with energies exceeding 100 GeV.

We can also take a look at the energy spectrum of neutrinos, illustrated in Figure 4.6. We see that most of the neutrinos have low energy, about 60% of them below 10 GeV. However, from this plot and the last one, we see that the low-energy neutrinos generate many fewer physics hits individually, as we will see in the next section. This will make them very hard to detect.

[1]In fact, the exact physical flux used is not of much importance here. We will use the rate from the noise, and the weight here is therefore only used to weight the low and high energy events together. As long as the spectrum is consistent, it will not change any results.

| Type | Rate |
|---|---|
| Noise | 6.30 MHz |
| Electron neutrino | 1.51 Hz |
| Electron anti-neutrino | 0.98 Hz |
| Muon neutrino | 1.66 Hz |
| Muon anti-neutrino | 1.11 Hz |
| Tau neutrino | 0.79 Hz |
| Tau anti-neutrino | 0.39 Hz |

Figure 4.4: Expected hit rates for the noise and the different neutrinos. The noise hit rate is six orders larger than the neutrino hit rates, due to the low rate of interacting neutrinos.

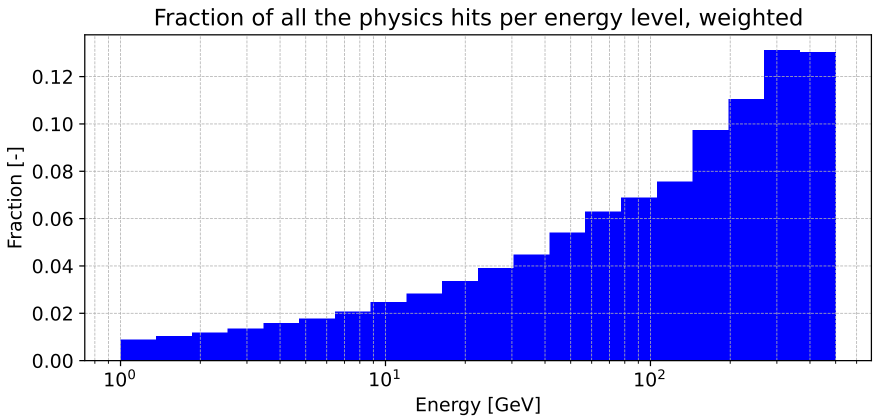


Figure 4.5: Spectrum of hits and energy, after the weighting, using a logarithmic energy scale. Most of the hits come from neutrinos with energies exceeding 100 GeV, as these are much larger events.

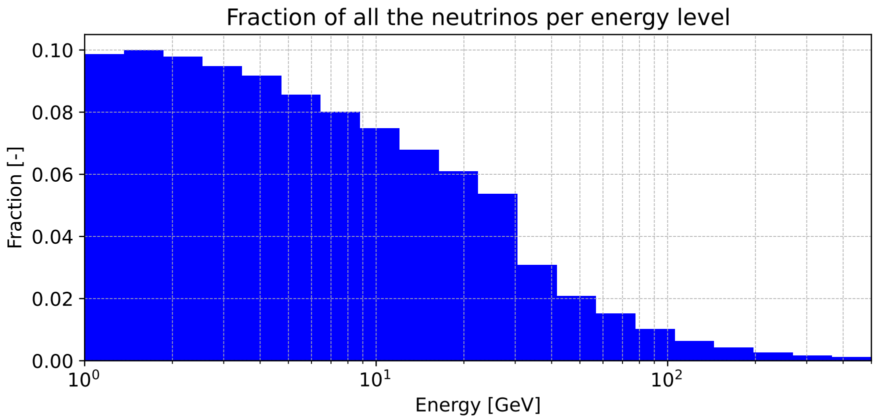


Figure 4.6: Spectrum of neutrino energy (after the weighting). Most of the neutrinos have a low energy, about 60% of them below 10 GeV. However, these low-energy neutrinos generate very few physics hits, making them hard to detect.

## 4.4 Number of hits per neutrino

Indeed, the last information that could be useful is the number of physics hits generated per interacting neutrino. We have already observed from the last section that the high-energy hits seemed to generate more physics hits. This is clear in Figure 4.7, as the number of physics hits is between 1 and 2 for neutrinos with energy smaller than 5 GeV.

This will be a problem as these hits are impossible to analyze, even with more complex, machine-learning-based algorithms. In the case of the LC pre-trigger, they will be mostly ignored as their small signal can't be distinguished from noise.

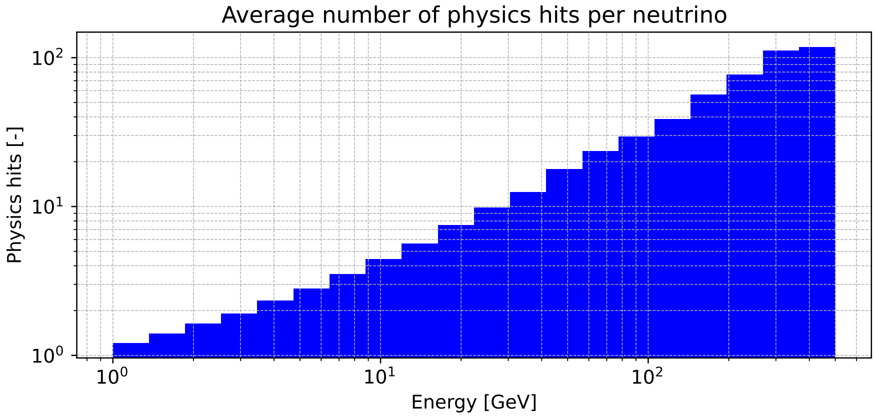


Figure 4.7: Average number of physics hits per neutrino, depending on the energy level, using a logarithmic scale for energy and number of physics hits. We see that the number of physics hits is much smaller for low-energy neutrinos. The neutrinos below 10 GeV generate a few physics hits each, and most of them won't be detectable anyway.

We can see this even more clearly if we impose conditions on the number of physics hits generated per neutrino. In Figure 4.8, we see for each energy level the fraction of neutrinos that generate at least 1,2, and 5 physics hits. About 36% of the neutrinos do not generate any physics hits (the neutrino interacts outside of the IceCube Upgrade array and is not detected at all). Of course, in the analysis later, we will not take these neutrinos into consideration. We also see that the fraction of neutrinos drops low with the number of physics hits required (47% for 2 physics hits, 31% for 5, etc.). This is summarized in Table 4.1. The fraction is especially low for low-energy neutrinos, where it rapidly drops to about 10%. Of course, these neutrinos will be very hard to reconstruct in post-processing using only the Upgrade data.

The fact that some neutrinos don't generate physics hits or generate only a few is due to the way the simulations are generated: the neutrinos interact in a cube of ice much larger than IceCube itself, and therefore sometimes only a small fraction of light arrives to the optical modules. Furthermore, here we only consider the IceCube Upgrade modules, which means that some of these neutrinos with a small number of hits in fact trigger modules in the current IceCube array.

| Minimum number of physics hits generated | Percentage of neutrinos |
|---|---|
| 1 | 64.28 % |
| 2 | 47.09 % |
| 3 | 39.18 % |
| 5 | 30.73 % |
| 10 | 21.43 % |
| 15 | 17.11 % |

Table 4.1: Percentage of neutrinos depending on the minimum number of physics hits generated. Most neutrinos generate only a few physics hits (36% of them don't even generate any), and will therefore be really hard to detect anyway.

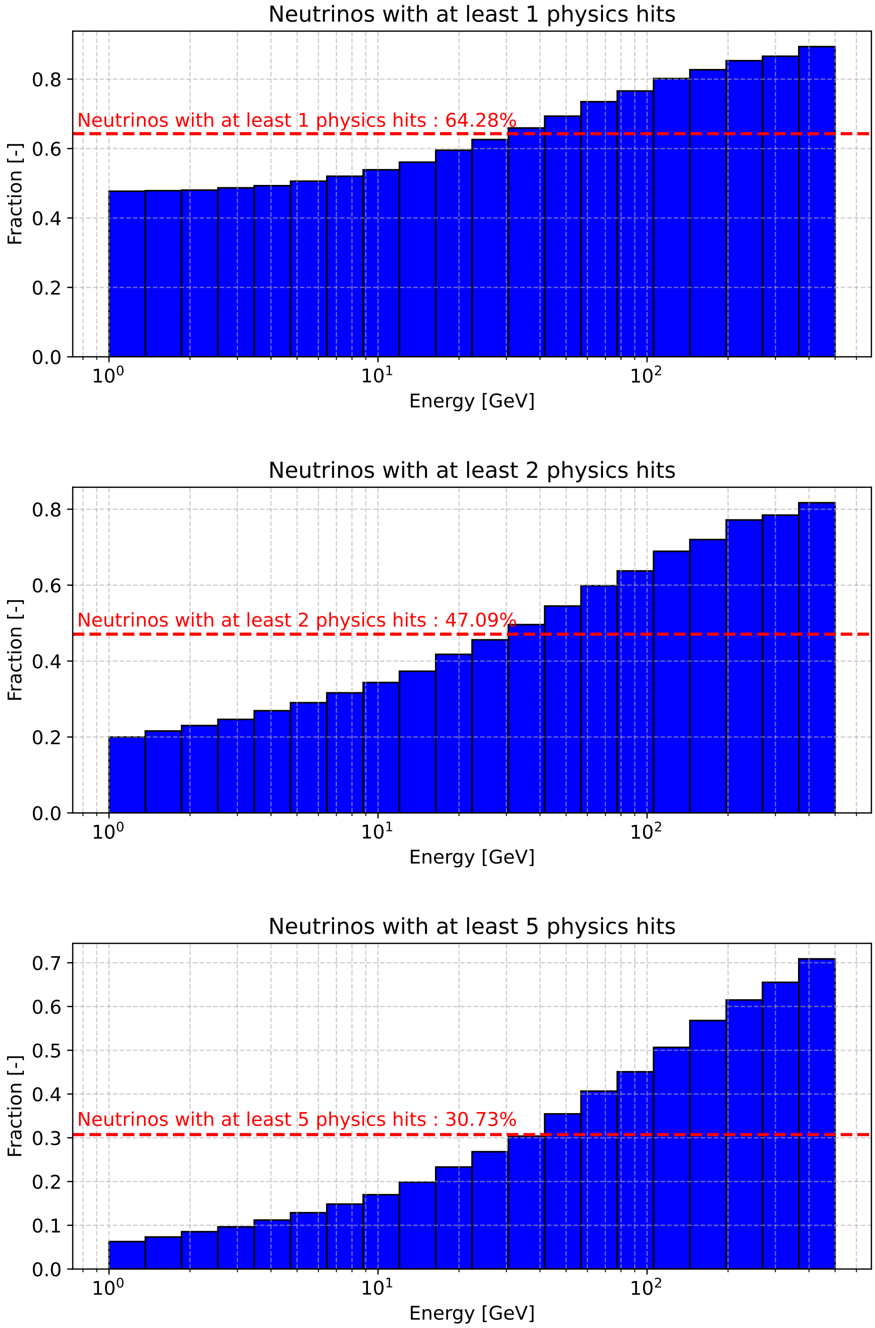


Figure 4.8: Fraction of neutrinos with at least 1, 2, and 5 physics hits generated in the IceCube Upgrade array. We see that even for one physics hit, the overall fraction is quite low (about 36% of neutrinos don't generate any physics hit in the Upgrade). At low energy, it is even worse: only about half of the low-energy (less than 10 GeV) neutrinos generate a physics hit, and this fraction drops to 10 to 15% for the low-energy neutrinos generating 5 physics hits.

## 4.5 Visualization

It can be useful for the creation and analysis of the trigger to visualize what the hits look like. To do so, a little code was implemented, where the hits are shown in the optical module where they come. Figure 4.9 shows the hits for low (8.35 GeV), middle (70.85 GeV), and high (283.43 GeV) energy neutrinos. We can observe that the number of hits increases with the energy of the neutrino, and the overall density too, as we have already seen in previous sections. Another observation is that the time between the first and last hit is at most about 2000 to 3000 ns, which will be useful for the pre-trigger condition later.

## 4.6 Differences between the sensor types

In the Upgrade, there are 3 types of modules: the PDOMs, which have only one PMT, the DEggs which consist of 2 PMTs, one up and one down, and the mDOMs which contain 24 PMTs. Of course, for the LC pre-trigger, it is important to see the differences between these sensors, as the behavior of the pre-trigger might depend on it. We will use both the noise and the neutrino files to do so. The idea is to understand what fraction of the physics hits come from each sensor, how much of it comes from noise and neutrinos, etc.

Figure 4.10 contains a lot of information. The rates are separated between the 3 types of optical modules. The percentage in parentheses is the fraction of all the hits that originate from this optical module, and next to it the corresponding rate. The number below is the fraction of those that are physics hits and the corresponding rate. The blue percentage represents the fraction of all the physics hits that come from this type of optical module. As expected, the PDOMs have little to no impact on the global rates or the physics hits, as they will be mainly used for recalibration and comparison with the DOMs already on IceCube. We see that the rate from the DEggs is much lower than the mDOMs, but more than a third of the physics hits come from them. Since the main goal is to get a rate lower than 3 MHz, the pre-trigger condition should mainly focus on the mDOMs.

From this chapter, we have observed from the simulations how the neutrinos are expected to generate physics hits in the IceCube Upgrade. From all this, there are a few main informations to take. First, high-energy neutrinos generate much more physics hits, and this can be extrapolated to energies even higher than 500 GeV. We have also seen that most of the low-energy (below 10 GeV) neutrinos generate close to no physics hits, meaning they will be hard to detect. There is also a large part, 36% of neutrinos, that doesn't generate any physics hits, and this phenomenon occurs even at high energy because we only consider the IceCube Upgrade array and not the rest of the detector. There is also a large part of the neutrinos that generates only a few physics hits, for the same reason. Finally, we observed that the optical modules do not behave similarly: the PDOMs and DEggs generate less noise relative to their physics hits rate, compared to the mDOMs.

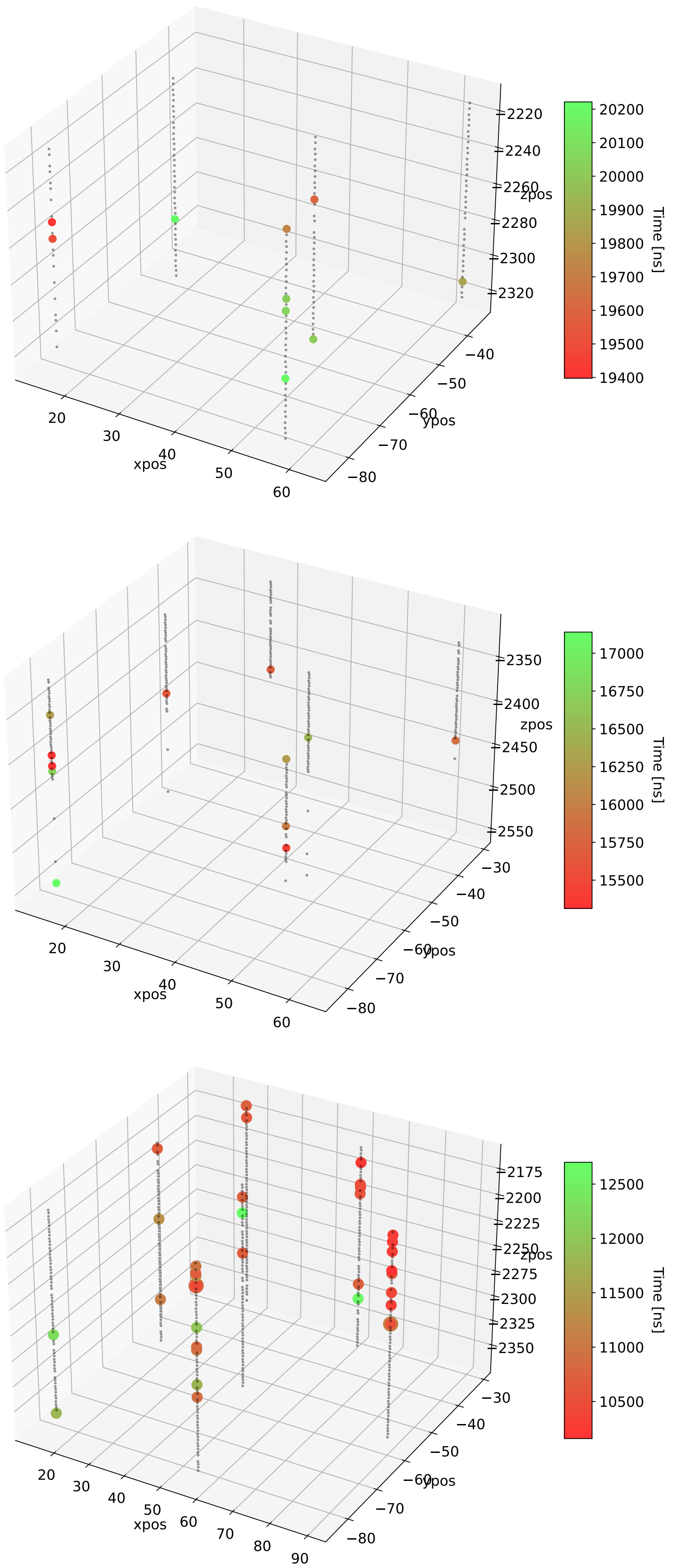


Figure 4.9: Visualization of physics hits for low, middle, and high-energy neutrinos. The black dots are the optical modules without hits, the color indicates the time of the hits and the size the number of hits. The number of physics hits increases with the energy of the neutrino, as we had already seen in previous plots. We can also observe that the maximum time between two physics hits seems to be about 2000ns, which will be useful later for the pre-trigger condition.

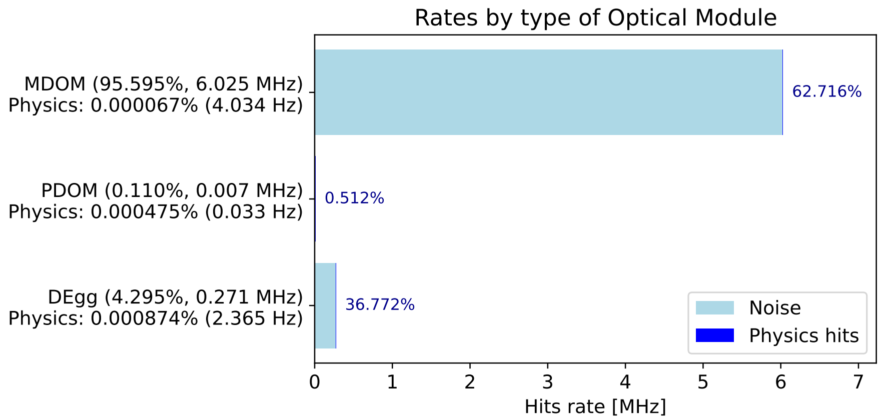


Figure 4.10: Noise and physics hits rates depending on the type of optical module. The deep blue numbers correspond to physics hits: 62% of them originate from mDOMs, 36% from DEggs, and only 0.5% from PDOMs. On the left, for each type of module, we see the percentage of all the hits (including noise and physics) that originate from them, with the corresponding rate. The numbers below indicate what the fraction of physics hits in this rate, and the corresponding rate of physics hits. We can observe that the PDOMs and DEggs generate less noise proportionally to their physics hits, compared to the mDOMs. This is especially interesting for the DEggs that generate only 0.27 MHz of noise while generating 37% of the physics hits. This will be specially used for the pre-trigger LC conditions.

# Chapter 5

# Pre-trigger propositions

In this chapter, we will propose and study multiple algorithms for the Local Coincidence pre-triggering. We will discuss the behavior between PMTs and the difference between PDOMs, mDOMs, and DEggs. The important parameters will be detailed after that.

As explained in Chapter 2, the original Local Coincidence pre-trigger in IceCube checks for the neighboring DOMs, with a time window between two hits of 1 ns. From what we observed in the last chapter, the same idea could be applied to the Upgrade. However, the main difference comes from the fact that in the Upgrade, the DEggs and the mDOMs have multiple PMTs. The pre-filter will also be applied by a computer instead of the hardware connection in the current IceCube. Therefore, a more comprehensive filter can be applied, where the behavior between PMTs on the same DOM and different DOM can be different, the behavior can depend on the type of DOM, and this filter can rely on much larger spatial and temporal distances. However, it also means that our condition can only depend on hits from the same string: it is not possible for a computer to access another computer's data. Of course, for all the methods here, the modules we only consider the Upgrade (ie. not the current IceCube array), and we ignore the modules that are not PDOMs, mDOMs, or DEggs, such as calibration devices.

## 5.1 First criterion: the fraction of physics hits retained

To characterize and study our filters, we first need a good way to estimate their results. Here, the simplest will be called the fraction of physics hits retained. It is simply the ratio between the physics hits that are categorized as LC and all the physics hits, which we can call the efficiency or retention rate of our filter. Of course, this value is different for each simulated neutrino, and we will use averaged values. For this chapter, only the files with electron neutrinos will be used as a preliminary design.

$$\epsilon_{\text{LC}} = \frac{\#LC\ physics\ hits}{\#physics\ hits}$$

## 5.2 Using a simple PMT condition

For the first version of the algorithm, a simple LC condition was used: on each module (ie. multiple PMTs), we need at least 2 hits within a time window called $\Delta t_{\text{PMTs}}$. For the DEggs and PDOMs, all the hits are LC as it would not be possible to have multiple hits, and we have already seen that they contained less noise. As we can see in Figure 5.1, even if this condition reduces the rate sufficiently, the fraction of physics hits that are LC tagged is quite low, just over 50 to 60%. After that, the rate increase is too large, and the fraction does not increase as much.

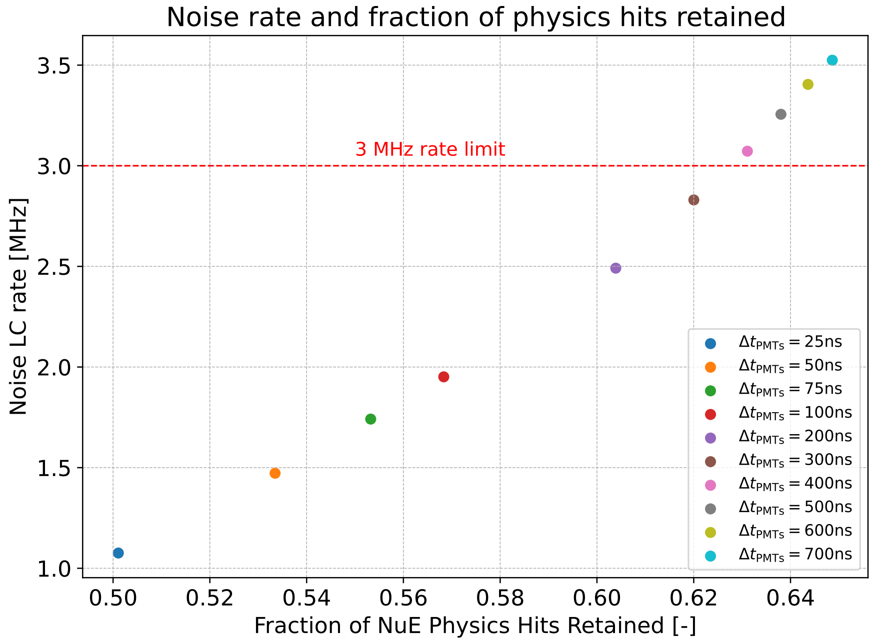


Figure 5.1: Noise rate and fraction of physics hits retained using the first pre-trigger with electron neutrinos. For a noise rate of about 3 MHz, we get a fraction of hits retained of about 62%. This rate is not satisfactory, and we will find better conditions to improve it.

## 5.3 Adding a neighbor condition

A second version that was tested implemented another condition with the first one: once the hits are validated (or not) using the first condition explained before, we check again if there are multiple valid pulses within the $n$ neighbors up and down (for greater clarity, we will call this parameter "LC span".), within a time window $\Delta t_{\text{DOMs}}$. The idea here was to keep the fraction high enough while lowering the rate (for the same $\Delta t_{\text{PMTs}}$), and see if we could increase the values of all the parameters to get a better fraction with the same rate. Of course, due to the proximity of PMTs in the same module compared to PMTs in different modules, the $\Delta t_{\text{PMTs}}$ should be smaller than $\Delta t_{\text{DOMs}}$.

The results in Figure 5.2 show that the fraction is reduced using this new filter, but the noise rate reduction is much larger. While this could be a good thing, it is however a problem: using the largest parameters, we only reach 50% of physics hits retained, which is not very large. Increasing the parameters further does increase the rate without increasing the fraction. While this pre-trigger could be of great use if we were limited to a lower rate, it is not efficient in our case. However, it indicates that the use of the neighboring hits is a way of improving the pre-trigger. The condition should be easier, and that is what will be done in the next section.

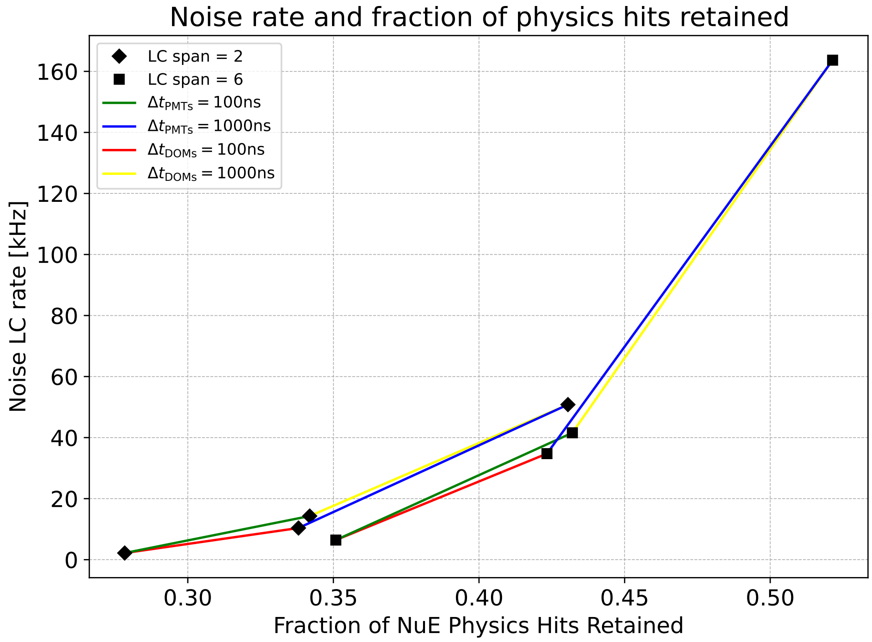


Figure 5.2: Noise rate and fraction of physics hits retained using the second pre-trigger condition with electron neutrinos. The colored lines show the $\Delta t_{\text{PMTs}}$ and $\Delta t_{\text{DOMs}}$ parameters used for each data point. In this case, the fraction is a bit reduced (some parameters reach about 52% of physics hits retained), but the noise rate is much lower, about ten times lower than with the first pre-trigger. This LC condition could therefore be used if a rate much lower than 3 MHz was needed.

## 5.4 Final version and relevant parameters

Now, the idea is to simplify the algorithm to allow more hits to be considered as LC. To do so, we will remove the first condition and only keep the second one. Now, for a hit to be LC, it needs to have at least one other hit within the $n$ neighbors up and down, and within a time window. Therefore, the PMTs on the same module are treated in the same way as those in the neighboring modules. Because the PMTs on the same module are much closer, it makes sense to apply a different time window when comparing two hits on the same module and different modules.

The results for this trigger are shown in Figure 5.3. We see that the fraction of physics hits retained is much larger than for the last pre-trigger, which is very good. Here, only a few sets of parameters are represented, but it is a good sign that we could optimize these parameters to reach larger fractions. We will do so in the next chapter, but before that, we can still improve this LC condition.

For the first improvement, we see in the simulations that, for the noise, there are a lot of hits that are doubled on the same PMT, within a very short time window. Therefore, a new parameter was implemented, which allowed us to consider the hits on the same PMT for the LC pre-trigger condition. For simplicity, we will call it **Same PMT**. If set to True, then when validating a hit as LC, it also considers the following hits on the same PMT. If No, then they are validated independently and do not trigger the LC filter for the previous hit. Once this parameter is set to False, the rate drops a lot, but the fraction is a bit increased (using a different set of parameters), as seen in Figure 5.4. We also see that the effect of the parameters is different, as the difference between the $\Delta t_{\text{PMTs}}$ has less effect.

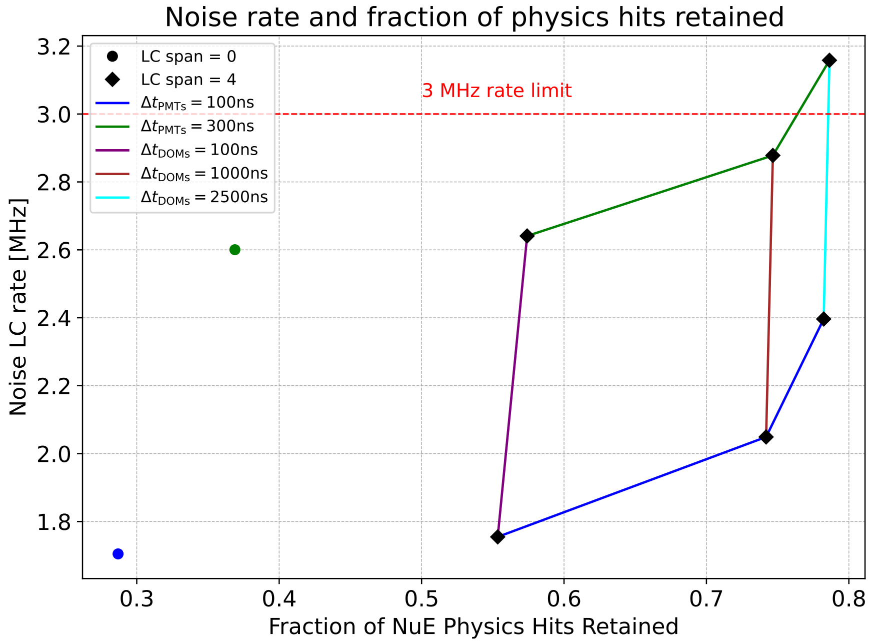


Figure 5.3: Noise rate and fraction of physics hits are retained using the last filter with electron neutrinos. The points with LC span = 0 are colored with the corresponding $\Delta t_{\mathrm{PMTs}}$. We see that some parameters retain more than 75% of the physics hits while having a noise rate lower than 3MHz. Furthermore, these parameters can be refined to get closer to a 3MHz rate and increase the fraction of physics hits retained. The $\Delta t_{\mathrm{PMTs}}$ parameter seems to be less efficient in improving the fraction retained, but it increases much more the noise rate.

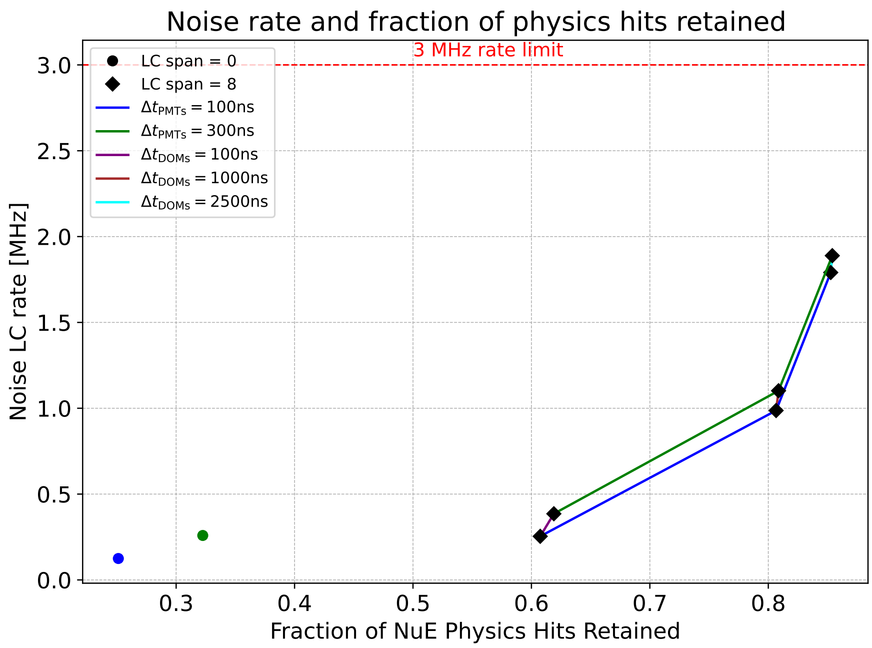


Figure 5.4: FFinal filter with **Same PMT** False. The rate is much lower with a larger fraction retained. It also changes the behavior of the $\Delta t_{\mathrm{PMTs}}$: before, it increased the noise rate without much increasing the fraction retained, and now it increases the physics hits retained more than the noise. This is a good sign that with optimal parameters, this pre-trigger condition could be better. This will be explored in the next chapter.

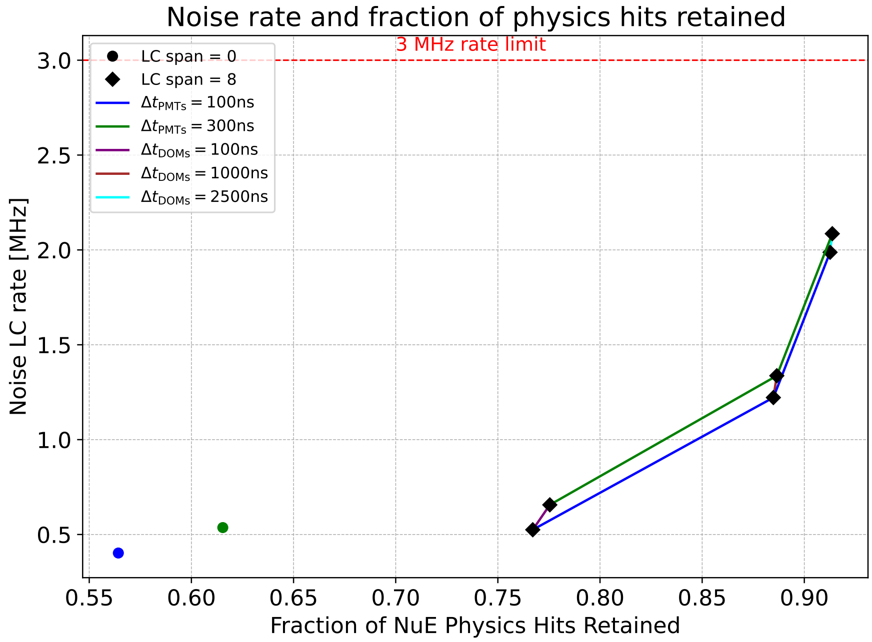


Figure 5.5: Final filter with **Same PMT** False and **DEggs/PDOMs** True. Compared to Figure 5.4, the fraction is a bit higher with a rate that is nearly the same. Again, this parameter increases the fraction, reaching values that we never reached before. Especially, this last parameter allows for single hits to pass the LC condition, which can be very useful at low energy.

Finally, we have seen in Section 4.6 that the noise was dominated at 95% by the mDOM hits, but that the PDOMs and DEggs were generating about 40% of the physics hits. Therefore, a last parameter was introduced to try to improve even more the fraction of hits retained. We will call it **DEggs/PDOMs** later. If set to True, then all the hits from the DEggs and the PDOMs are considered LC, without even checking for neighboring hits. It should be noted that these hits are still used when checking the neighbors. For example, if a DEgg has a hit and a neighboring mDOM also has a hit, both hits are LC. If only the mDOM has a hit, then it is not LC, but a DEgg hit alone is LC. As seen in Figure 5.5, we can increase the fraction of hits retained by using this new condition, while not increasing the rate as much. This is good, as the fraction reached has never been so high: easily more than 90%. Furthermore, we will see in the next sections that allowing for single hits to be considered LC can be very efficient at low energy.

## 5.5 Sanity check

The last algorithm was run using multiple sets of parameters or datasets as a sanity check, to be sure that it behaved well in simple cases. As we see in Figure 5.1, the results are what we should expect for these parameters. The only time we have a non-zero rate is when we set the **DEggs/PDOMs** to True, in which case we only have the rates of the PDOMs and DEggs, as we had seen in Figure 4.10.

| Same PMT | DEggs/PDOMs | $\Delta t_{PMTs}$ | $\Delta t_{DOMs}$ | $n$ | Rate | $\epsilon_{\text{LC}}$ |
|---|---|---|---|---|---|---|
| Yes | Yes | 0 ns | 0 ns | 0 | 277.6 kHz | 38.01% |
| Yes | Yes | 0 ns | 0 ns | 4 | 277.6 kHz | 38.01% |
| Yes | No | 0 ns | 0 ns | 4 | 0 Hz | 0.00% |
| No | Yes | 0 ns | 0 ns | 4 | 277.6 kHz | 38.01% |
| No | No | 0 ns | 0 ns | 4 | 0 Hz | 0.00% |

Table 5.1: Parameters and results used for the sanity checks.

# Chapter 6

# An analysis of the results

From the last chapter, we have found a suitable way to filter the hits from the optical modules. We have identified multiple parameters that we can vary. Now, we will analyze how the hits are filtered in a more comprehensive way, depending on these parameters.

For the analysis, we will define three energy levels to categorize neutrinos: low-energy, from 1 to 10 GeV, mid-energy, from 10 to 100 GeV, and high-energy from 100 to 500 GeV. This will be useful to show some numerical values.

## 6.1 Global rate and fraction of physics hits retained

First, the trigger was run with hundreds of combinations of the parameters. Some of these sets are illustrated in Figure 6.1. We see that increasing $\Delta t_{\text{PMTs}}$ increases the rate much more than the fraction of physics hits retained while increasing $\Delta t_{\text{DOMs}}$ does the inverse. Finally, up to a certain point, increasing the LC span is a good way of increasing the fraction without increasing the rate as much. However, when the **Same PMT** condition is set to False, increasing $\Delta t_{\text{PMTs}}$ has much better efficiency, as we can see in the two bottom graphs.

Then, we can identify the sets with a rate lower than 3 MHz and a high ratio of physics hits retained. Four of these sets are detailed in Table 6.1. As we see, they all reach about 90% of physics hits retained or more. We also see that sets 1 and 3 globally seem to be better. With these four sets, we will conduct a more thorough analysis to find the best-suited set for the pre-trigger[1] In particular, we will use a much larger simulation dataset (about 20 times) to get more accurate values.

| ID | **Same PMT** | **DEggs/PDOMs** | $\Delta t_{PMTs}$ | $\Delta t_{DOMs}$ | $n$ | Rate | $\epsilon_{\text{LC}}$ |
|---|---|---|---|---|---|---|---|
| 0 | Yes | Yes | 5 ns | 2500 ns | 12 | 2.76 MHz | 94.10% |
| 1 | Yes | No | 5 ns | 2500 ns | 12 | 2.6 MHz | 90.44% |
| 2 | No | Yes | 300 ns | 2500 ns | 12 | 2.73 MHz | 93.93% |
| 3 | No | No | 100 ns | 2500 ns | 16 | 2.96 MHz | 91.99% |

Table 6.1: The four sets of parameters were chosen for the following analysis. The sets 0 and 2 have larger efficiencies because of the **DEggs/PDOMs** parameter, which is very efficient in increasing the physics hits retained. We will see in this section the reason for this.

[1]It should be noted that if the rate needed at the end is lower or higher than 3MHz, or if a safety factor is implemented, then the set of parameters should change accordingly. The tendencies and various observations in this analysis would still hold, only with small variations in the numerical values.

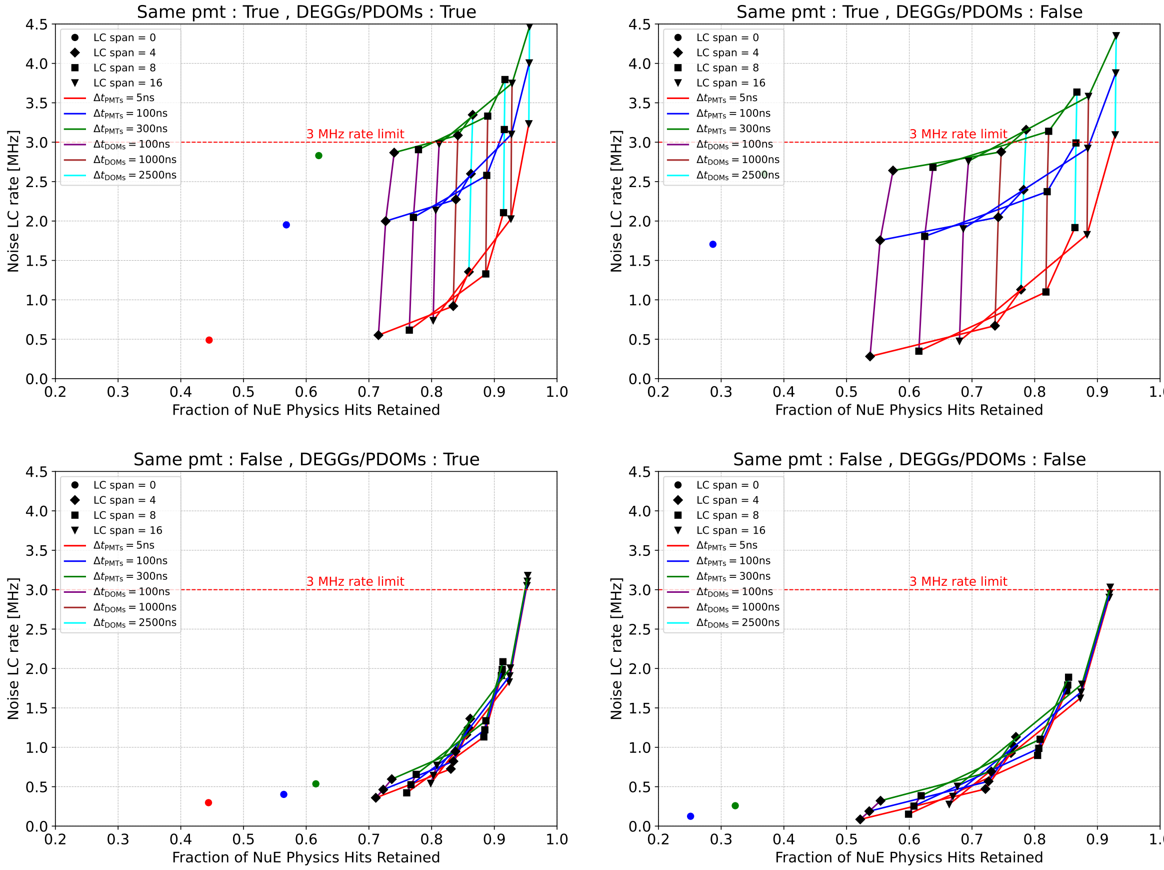


Figure 6.1: Rate and fraction of physics hits retained, for multiple sets of parameters. On the top left, we have **Same PMT** and **DEggs/PDOMs** set to True. On the top right, it is True/False, False/True on the bottom left, and False/False on the bottom right. We are able to reach a rate lower than 3 MHz with a fraction of physics hits retained larger than 90%, which is pretty good. We can see that in the left column, when **DEggs/PDOMs** is True, the results are globally better, and we reach a higher fraction. On the bottom line, we see that the behavior changes when we set **Same PMT** to False, as the impact of the $\Delta t_{\mathrm{PMTs}}$ parameter is more useful than before.

## 6.2 Incident neutrino energy dependence

Intuitively, we expect that a more energetic neutrino should trigger much more hits on the optical modules. The LC pre-triggering for these high-energy neutrinos should be easier to detect, as they would lead to a lot more hits, probably closer to each other spatially and temporally. Therefore, the efficiency of the pre-trigger could vary a lot with the neutrino energy.

In this section, we will see how the condition behaves, using the four sets of parameters defined in Figure 6.1, depending on the energy level. In each figure, the parameters used are written. The bars represent the fraction of physics hits that are retained for this energy level, and the average value (weighted) is drawn with a red dotted line. As we see in Figure 6.2, the trigger efficiency using the larger dataset for the first set of parameters is 95.69%. As we expected in the analysis of the simulation, the efficiency is larger for high-energy neutrinos: more than 95% for neutrinos with an energy greater than 70 GeV. The few hits that are lost are due to the neutrinos interacting mostly outside of the Upgrade array (for example, about 5 to 10% of the high-energy neutrinos generate only one physics hit, which is hard to detect). This fraction drops lower, at about 80%, for neutrinos with energy in the range of a few GeV. The fact that the fraction increases with energy means that we can extrapolate this for neutrinos with $E > 500GeV$, and we have an efficiency close to 100% for these.

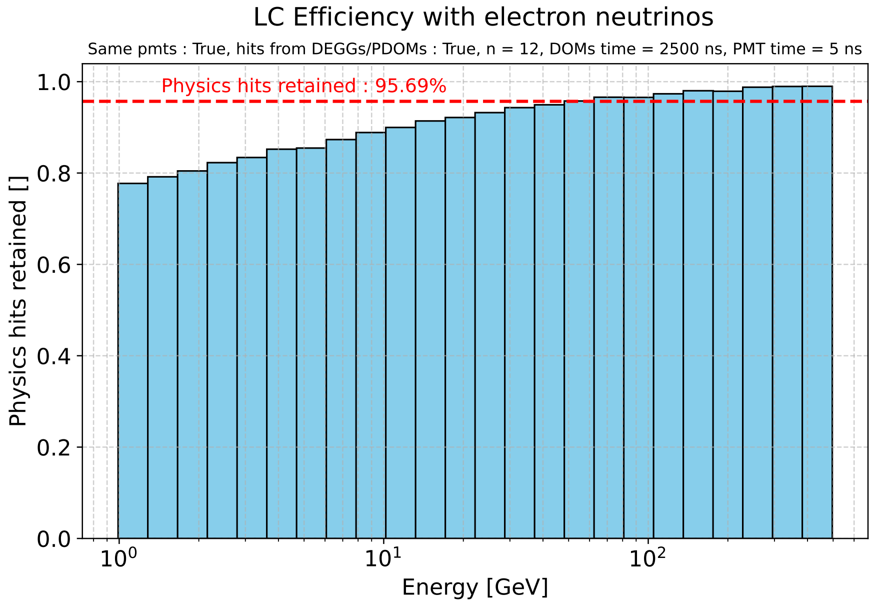


Figure 6.2: Fraction of physics hits retained as a function of the neutrino energy for the first set of parameters. As expected, the efficiency is larger for high-energy neutrinos. More than 95% of physics hits are retained at this energy range. This fraction lowers at low energy but is still always above 80%, which is very good, and much better than what we could have had with the other previously suggested filters.

In Figure 6.3, the same distribution is presented for the four sets of parameters presented before. We see that all efficiencies are higher than what we had measured in the limited dataset, which is positive. However, the efficiency drop observed at low energies is much larger when the overall efficiency is lower, even if this last difference is small. For example, between sets 0 and 1, the efficiency change is only 4%, but it is mostly at low energies, where the best parameters have an efficiency of about 80%, while only 65% for the second one. In particular, the parameter **DEggs/PDOMs** seems to have a big impact on the results at this level. This can be explained: we have already observed that there are very few hits at this level of energy. Therefore, the fact that this parameter allows for single hits to be LC can dramatically increase the efficiency at low energies. At higher energies (approximately 100 GeV), the results are generally the same.

However, the value used here to describe the filters is not very accurate: for example, if a neutrino generates 15 physics hits, missing one should not be a big deal. Using a more complex algorithm or machine learning in post-treatment, it is probably possible to reconstruct the neutrino even if a few hits are missing. Therefore, it is much more important to see how many hits we keep for each neutrino. Simply said, it is much better to keep 100% of neutrinos, each with 90% of their hits, than to keep 90% of neutrinos, each of them with 100% of their hits, but this gives the same LC efficiency. We will here define a new value to characterize the filter, the Minimum Hit Fraction Efficiency $\epsilon_{\geq x\% \text{ hits}}$, the fraction of neutrinos for which at least $x\%$ of the physics hits are categorized as LC.

$$\epsilon_{\geq x\% \text{ hits}} = \frac{\#neutrinos\ with\ at\ least\ x\%\ physics\ hits\ as\ LC}{\#neutrinos}$$

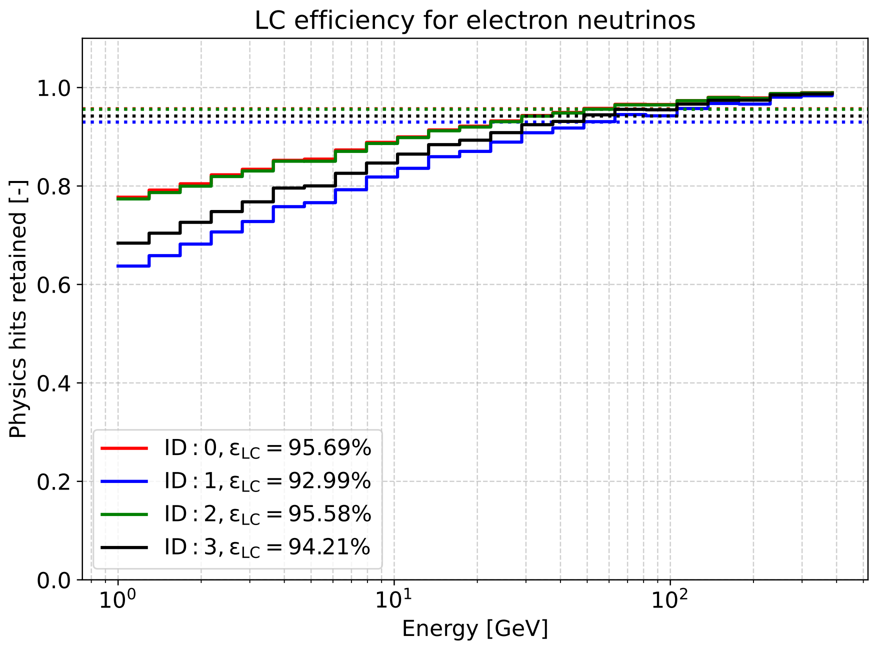


Figure 6.3: LC efficiency for the four sets of parameters used for the study. The efficiency is lower for low-energy neutrinos, especially when the **DEggs/PDOMs** parameter is set to False. Still, using the two best sets, the pre-trigger condition is fulfilled by more than 80% of the low-energy physics hits, which is large enough, considering the large part of neutrinos having only a few physics hits at this energy level. This is the reason why the **DEggs/PDOMs** parameter is efficient: it allows for single physics hits to be considered LC, and therefore increases the fraction, especially at low energy.

The Minimum Hit Fraction Efficiency is shown in Figure 6.4, with 50, 75, 90, and 100% values. The efficiency is quite high: for more than 80% of the neutrinos, we keep at least 50% of the physics hits (with the best parameters). For about 40% of the neutrinos, the pre-trigger retains all the physics hits. At $x = 100\%$, the fraction decreases with energy: the reason for this is probably because, at high energies, some photons can travel further and therefore trigger single PMTs in other parts of the detector, and these hits might not be categorized as LC, similarly to what happens at low energy. Again, at low energies, the pre-triggers using **DEggs/PDOMs** True get better results. However, the average Minimum Hit Fraction Efficiency is also much higher for these LC conditions, which indicates that this criterion is very efficient in distinguishing the best parameters.

Appendix A contains detailed plots of all the numerical values of efficiencies at low, mid, and high energies. For high-energy neutrinos, it confirms that all the parameters yield very similar results. However, low-energy neutrinos have much higher efficiencies for sets 0 and 2, because of the **DEggs/PDOMs** parameter used.

In this section, we see that the trigger has a very high efficiency. This can vary depending on the efficiency that we measure, but globally, we can expect to be able to reconstruct a lot of the neutrinos. In Figure 6.5, we can see a graph of all the values for the different sets of parameters. While the overall LC efficiency is close for all the parameters, about 93-95%, the Minimum Hit Fraction Efficiency shows another picture, with sets 0 and 2 being much more efficient. An interesting feature for the installation of the Upgrade is that the first and third sets of parameters have very close results but do not work in the same way (in one case, the hits from the same PMT are ignored), which means that we

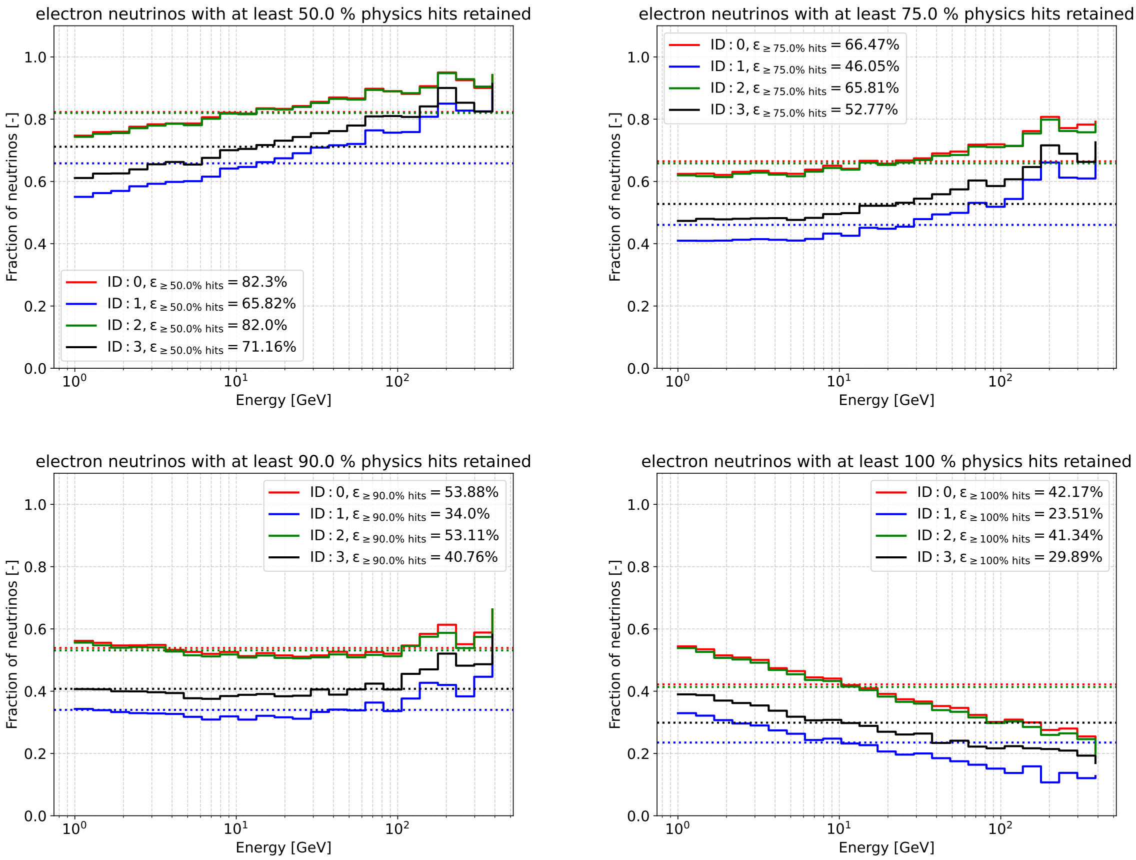


Figure 6.4: Minimum Hit Fraction Efficiency with 50,75,90 and 100%. The efficiency increases with energy, except at very high percentages (>90%). This is probably due to high-energy neutrinos generating photons that propagate further and trigger single physics hits that are not detected. The efficiency is high, with the best parameters there are 40% of the neutrinos that have 100% of their physics hits retained, and 80% of the neutrinos have at least 50% physics hits retained.

can choose the easiest-to-implement pre-trigger condition. Furthermore, as the efficiency of the detection increases with energy, we can extrapolate that we should be able to detect a very high percentage of neutrinos over 500 GeV with very high efficiency.

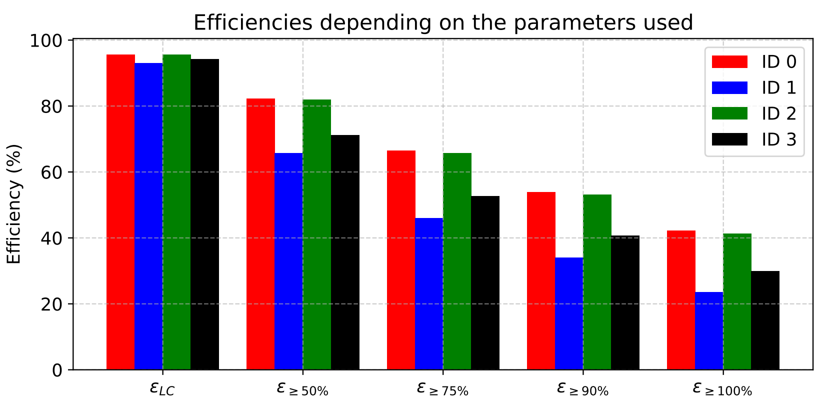


Figure 6.5: Efficiencies for the four sets of parameters. Sets 0 and 2 reach much better results and are very similar. For 40% of the neutrinos, the LC pre-trigger condition is fulfilled for all the physics hits generated by the neutrino. The Minimum Hit Fraction Efficiency is a better criterion than the LC efficiency, as it allows us to see more clearly that the parameters 0 and 2 get better results.

## 6.3 Influence of the neutrino type

For now, we only considered the electron neutrinos. However, as we have seen in Chapter 2 and particularly in Figure 2.3, the different types of neutrinos have different event signatures. This means that the efficiency of the trigger could vary depending on the neutrino type. In this section, we will compare the results of the filter for the six types of neutrinos.

For the LC efficiency $\epsilon_{\text{LC}}$, Figure 6.6 shows the value for each type of neutrino, depending on the energy. As we can see, we can't observe any major difference between any type of neutrino. The results are very close to each other, but most importantly, the trends are the same: the efficiency increases with energy, and it is larger for sets 0 and 2. This confirms the idea that these two sets are probably optimal.

Minimum Hit Fraction Efficiency is shown in Figure 6.7 for $x = 75\%$. As we had seen with the LC efficiency, the trends and results are again the same for each neutrino type: sets 0 and 2 get better results, the efficiency increases with energy, and the numerical values are roughly the same. The same plots for $x = 50\%$, $x = 90\%$, and $x = 100\%$ are shown in Appendix B. In all cases, the overall behavior of the LC pre-trigger condition is the same, which is good, as it will allow for a good detection of any of the neutrinos. The results being the same for all types of neutrinos, exact efficiencies at low, mid, and high energies were not computed, as they would result in very similar values to the ones computed shown in Appendix A.

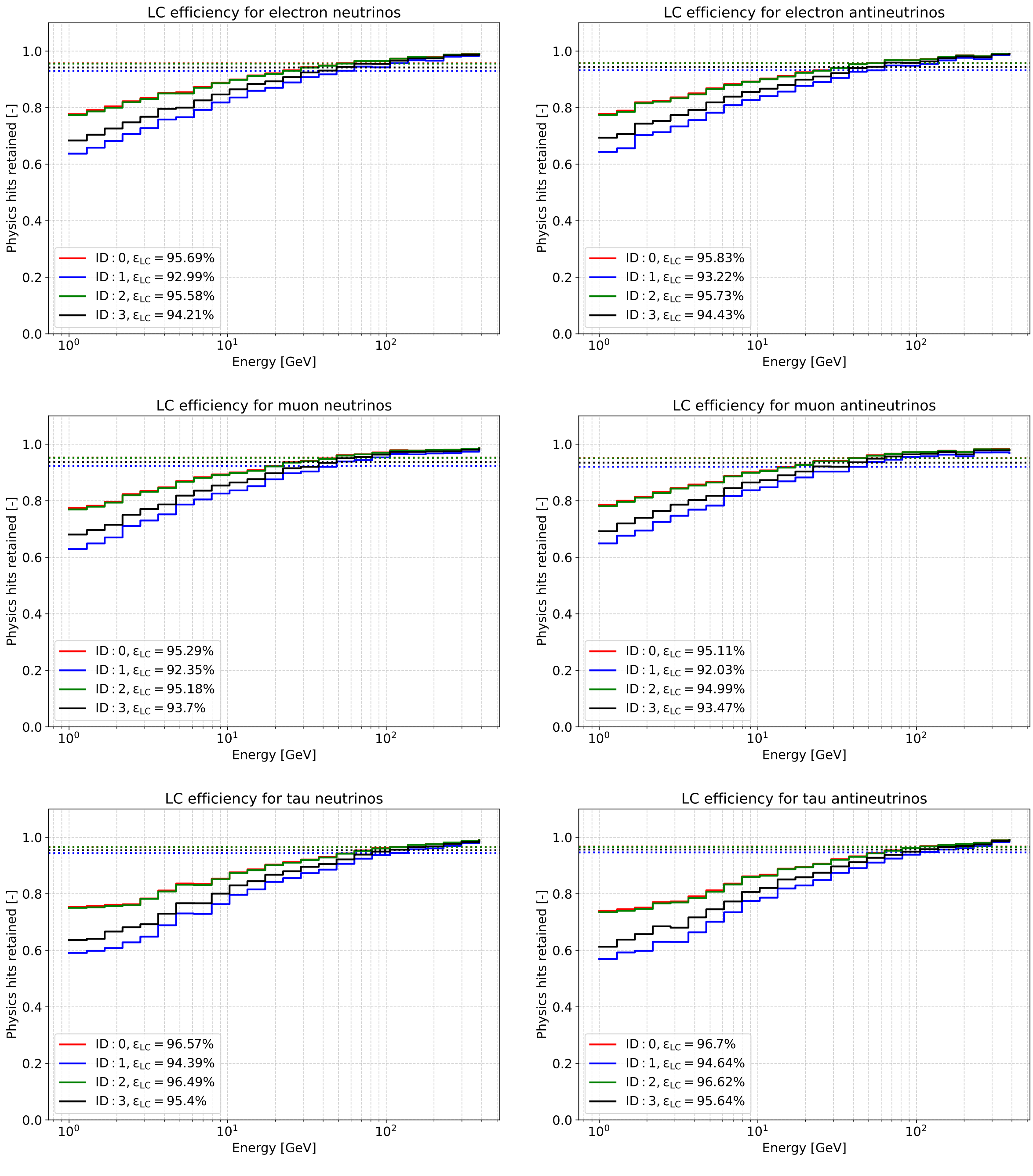


Figure 6.6: LC Efficiency for the four parameters sets, for each type of neutrino. The results do not change with the type, as the trends are the same: efficiency increases with energy, and sets 0 and 2 get better results. The numerical values change slightly, but these variations are negligible.

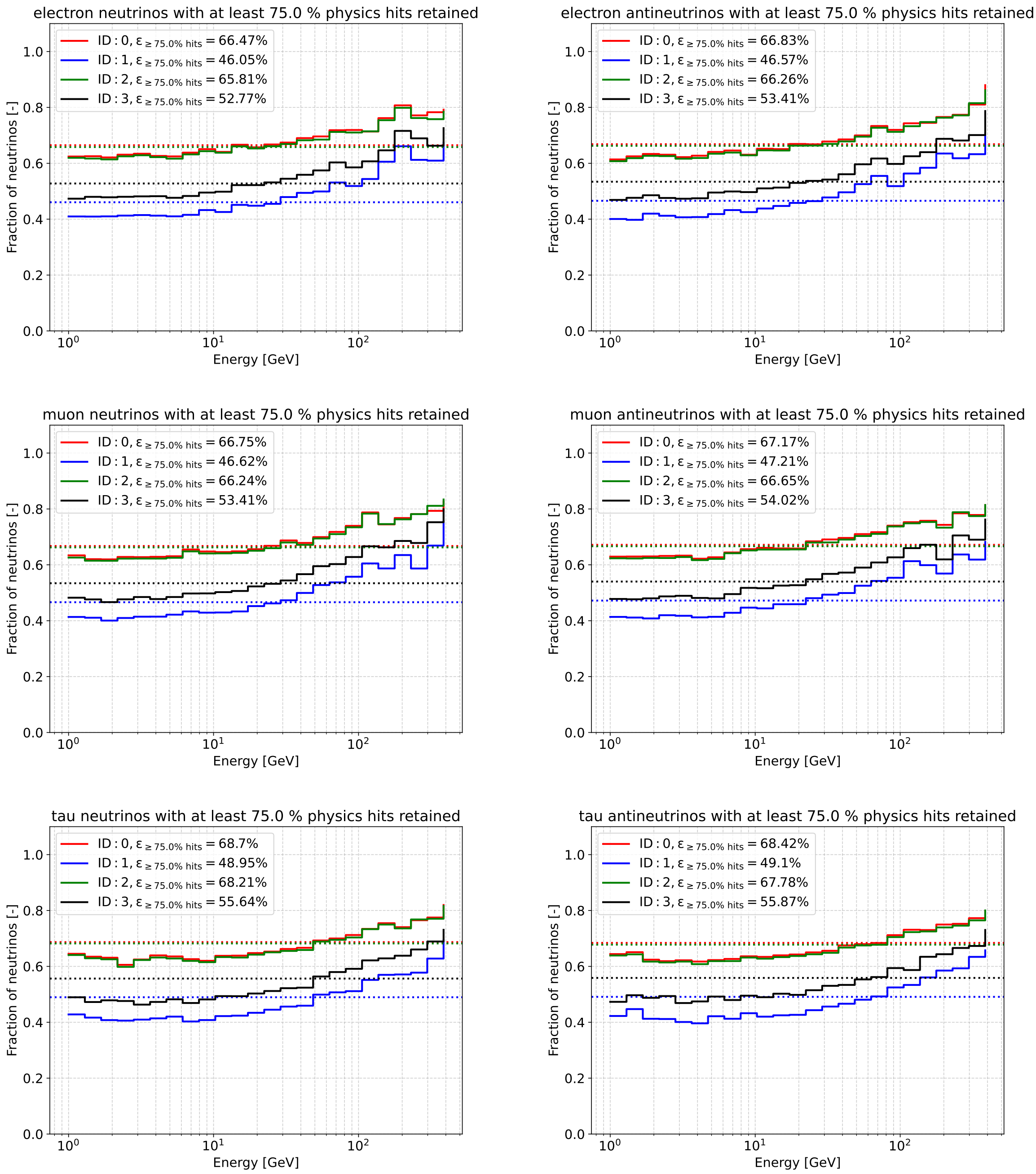


Figure 6.7: Minimum hit fraction efficiencies for the different types of neutrinos, here with $x = 75\%$. Other values are shown in Appendix B. The values and trends are the same for every file, which indicates that the pre-trigger LC condition will be efficient for all the neutrinos.

## 6.4 Visualization of the pre-trigger condition

Using the visualization tool defined in section 4.5, we can analyze how the hits are filtered depending on the neutrino energy and type. We will do it by analyzing electron neutrinos at low, mid, and high energies, only using set 0, which gives the best results.

### Low-energy neutrino

The low-energy neutrino used for the visualization is the one, with an energy of 7.77 GeV, shown in Figure 6.8. Even though this energy is low, it creates a large event in the IceCube Upgrade array with 59 physics hits generated, and will therefore be a good example of a low-energy neutrino that can probably be well reconstructed later. We see that only a single physics hit is lost on the rightmost string, reaching an efficiency of 98.3%. This event will therefore be easily reconstructed when applying higher-level algorithms.

### Mid-energy neutrino

For the mid-energy neutrino, we chose one with an energy of 42.54 GeV, with 45 physics hits generated. From it, only 3 are lost once the pre-trigger has been applied, which gives an efficiency of 93.33%. We can see them: one on the bottom of the leftmost string, one on the bottom of the third leftmost string, and one on the center of the sixth string. These are isolated hits on mDOMs. Still, the 42 remaining physics hits are enough to get information about the neutrino.

### High-energy neutrino

Finally, the high-energy neutrino represented in Figure 6.10 is a 106.51 GeV neutrino generating 76 physics hits. From this, 75 pass the pre-trigger LC condition, giving an efficiency of 98.7%. This lost hit is on the edge of the event and does not change it much. This gives results very similar to what we had earlier.

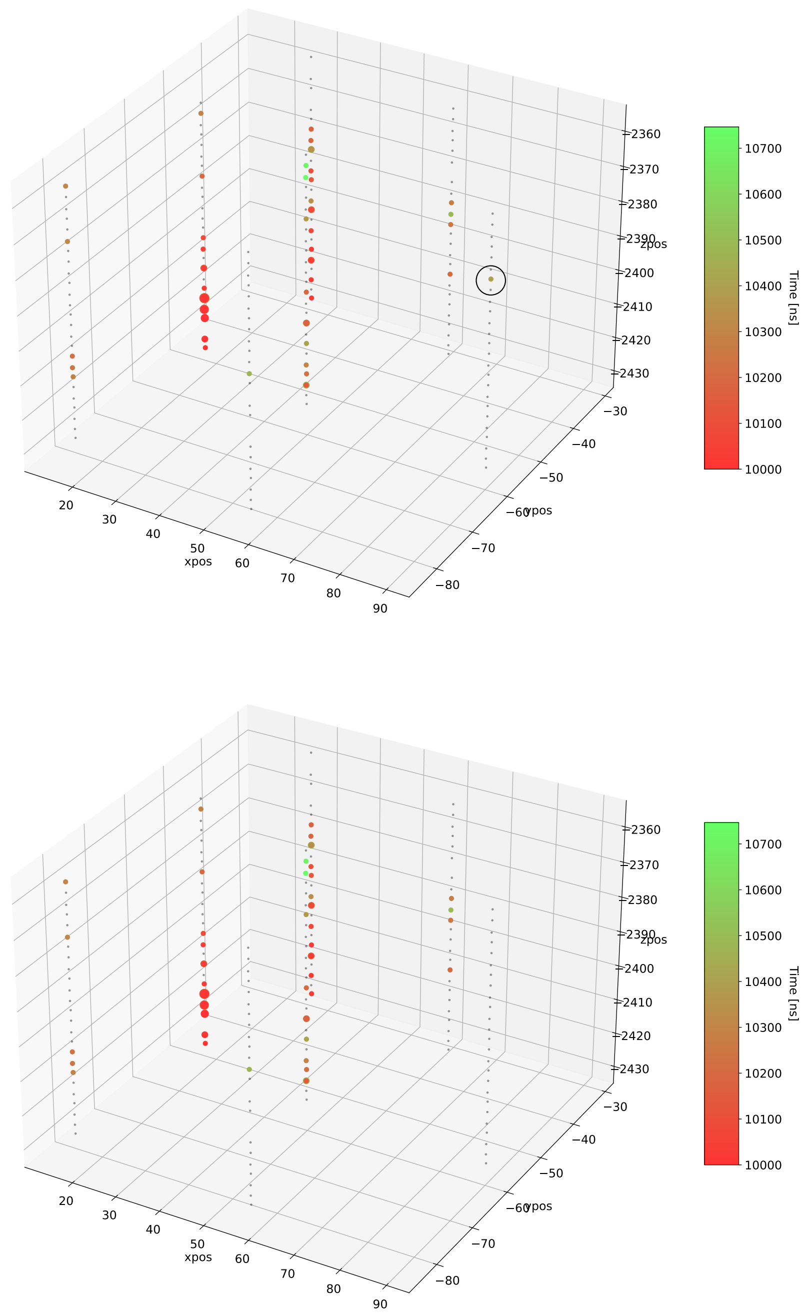


Figure 6.8: Low-energy neutrino (7.77 GeV) that creates a large event in the IceCube Upgrade array, before and after the LC pre-triggering. Only a single physics hit (encircled) is lost from the 59 generated, on the rightmost string. Therefore, the LC pre-triggering used here does not change much the event, which will be reconstructible later.

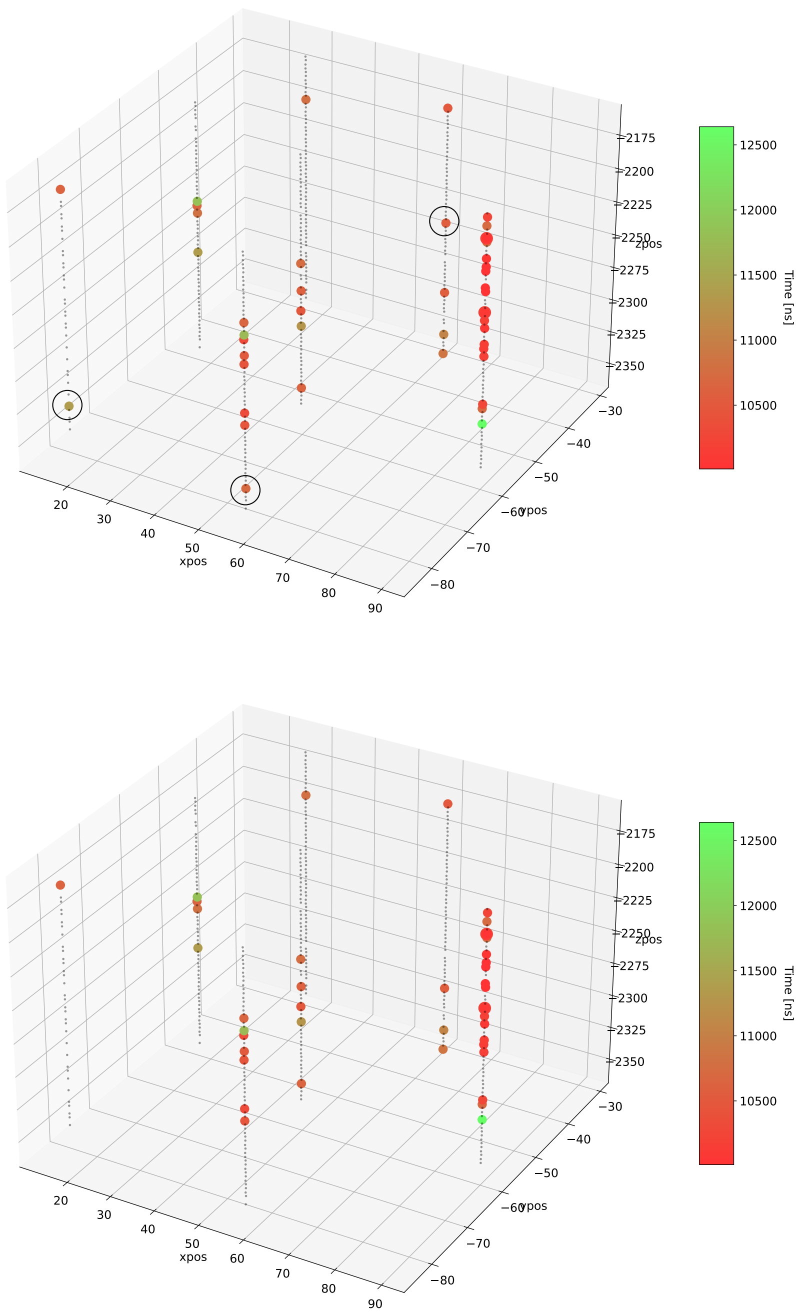


Figure 6.9: Mid-energy neutrino (42.54 GeV) with 45 physics hits generated. Only the 3 encircled hits are lost as they are isolated on mDOMs, giving a 93.33% efficiency. This fraction is still large enough, especially as the 42 physics hits detected are probably enough to reconstruct the neutrino correctly.

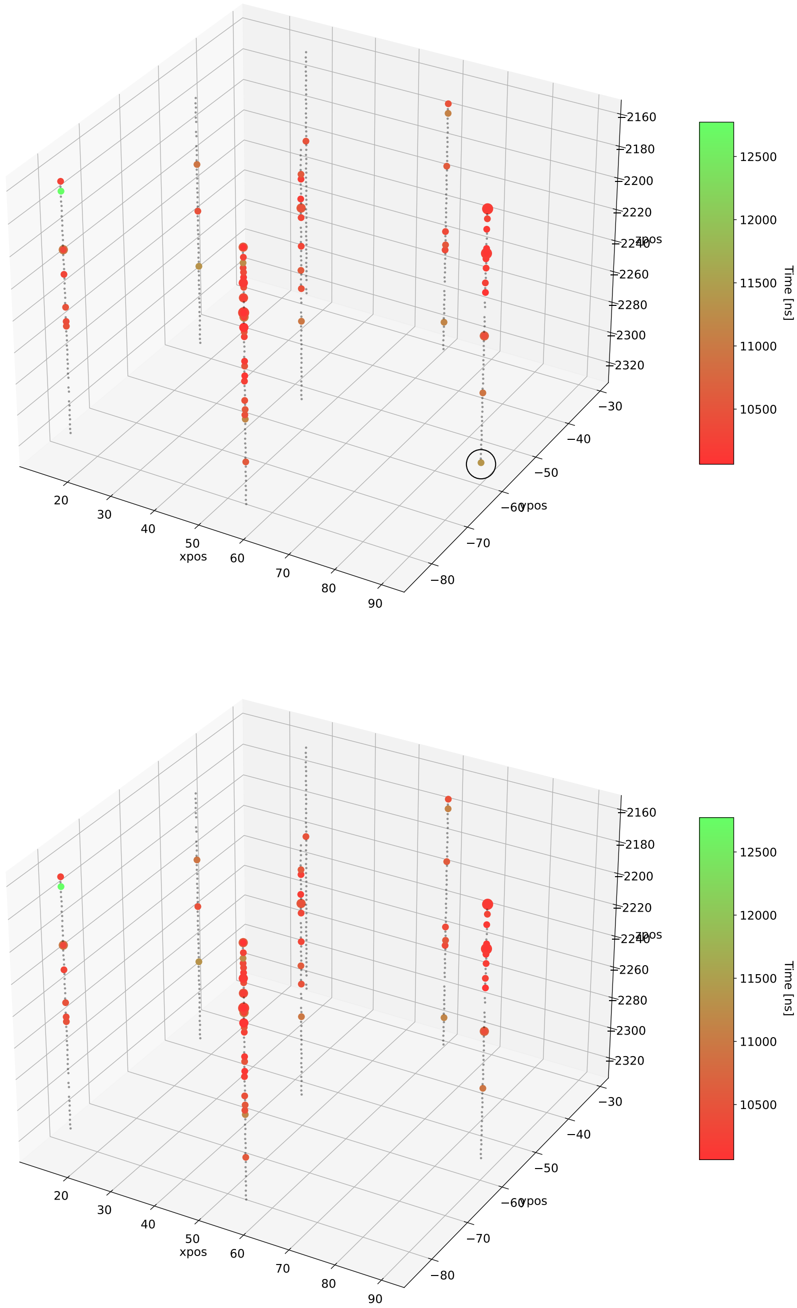


Figure 6.10: High-energy neutrino (106.51 GeV) event in the IceCube Upgrade array. From the 76 physics hits generated, 75 pass the LC pre-trigger, giving an efficiency of 98.7%. This large fraction and the large number of physics hits generated means that the neutrino is nearly perfectly detected, and the only lost hit is on the edge of the event.

This visualization shows something important: except for the neutrinos with only very few physics hits that are lost, in most cases, only a few physics hits are lost (1,2,...), which probably would not give much information about the neutrino (they are isolated spatially and temporally). The fraction obtained for the efficiency depends more on the physics hits first generated by the neutrino. This validates the pre-trigger LC condition, as losing only a few hits on some neutrinos should not be a problem for most of the neutrino reconstruction later. Of course, the neutrinos with very few physics hits are much more often lost or with low efficiency (for example, a lot of neutrinos generating two hits on the array, from which only one single hit passes the LC condition, won't be detectable using only the Upgrade data)[2]. To confirm this observation, Figure 6.11 shows the average number of physics hits lost by the pre-trigger. The average value is below one for the parameters 0 and 2, and even at high energy, this value reaches about 2.5 hits lost.

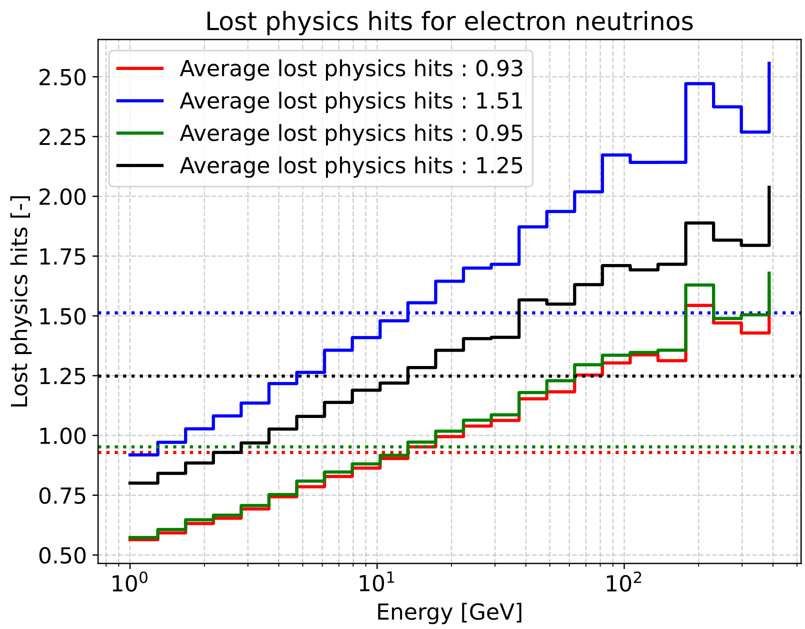


Figure 6.11: Number of physics hits that do not pass the LC pre-trigger condition. On average, about 1 hit is lost, and even at high energies, it is still at 2.5 hits lost, confirming what we had observed in the visualization: the number of hits lost is very low at any energy range, indicating a good choice for the pre-trigger LC.

Finally, we have shown in this chapter the very high efficiency of the pre-trigger LC condition proposed. In particular, at high energies, it keeps nearly all the physics hits from the neutrinos, and the few lost are due to neutrinos only slightly interacting in the IceCube Upgrade array, as we had described in Chapter 4.1. These neutrinos, which interact only slightly, will likely be detected using the IceCube array. From the results obtained, we can infer that this efficiency will be even better for neutrinos with energies exceeding 500 GeV, meaning that we can expect to detect neutrinos in a wider energy range than before with IceCube.

[2]It should be noted that, while the results here are shown with the first set of parameters, which gives the best results, they still hold for the third one, confirming that these two parameters sets are well-suited as pre-trigger LC conditions.

# My contribution

The first step in my master's thesis was to learn the IceTray software framework. This software, developed by the IceCube Collaboration allows for the generation, reading, and analysis of simulations and data for IceCube. I focused my efforts on reading the most recent simulation and geometry files corresponding to the IceCube Upgrade.

At first, I tried a few simple pre-trigger conditions that did not give good results. After that, I conducted a thorough analysis of the simulations, that I presented in this work. It allowed me to better understand how the neutrinos were interacting with the IceCube Upgrade array, what I could expect from the pre-trigger, etc. It also allowed us to show that some neutrinos could not be separated from noise due to the low number of hits that they generate.

Then, I implemented the trigger conditions presented in this work. It was based on what already existed for IceCube and on the results from my analysis done before. From this, I had five parameters that I could vary. After checking that the results were consistent with simple values (such as zero rates,...), I tested a few hundred different sets and chose the ones with the best efficiency while staying below the 3 MHz threshold.

I then analyzed the results for these best sets using the LC efficiency value and it gave similar results. To distinguish them, I defined a new value that was more representative of the objective of the pre-trigger. Using this, I showed that the results were very good and similar for each kind of neutrino. Finally, I showed that the pre-trigger is losing only very few hits for each neutrino, and its efficiency is especially high at energies close to 500 GeV.

The last step I did was to make this code usable again. I coded it like a module that can be implemented in IceTray, and can therefore be reused again with new simulations or parameters, for example, if a different limit rate is needed.

# Conclusion

In this master's thesis, the objective was to define a new pre-trigger Local Coincidence (LC) condition for the IceCube Upgrade, with the aim of reducing the hit rates to less than 3 MHz.

Initially, the thesis presents the IceCube Observatory and the IceCube Upgrade, including technical details about the current and planned detectors. The available simulations for the IceCube Upgrade were then analyzed in detail. The expected noise rate was found to be approximately 6 MHz, while the hardware limited the hit rate after the pre-trigger to about 3 MHz. It was observed that most neutrinos generated only a few or no physics hits in the IceCube Upgrade array, indicating that detecting these neutrinos using only the Upgrade would be challenging. A visualization of the events illustrated that the number of hits increased with energy.

In the subsequent chapter, several algorithms were proposed for the pre-trigger LC condition, leading to the identification of five important parameters. From the last proposed pre-trigger, hundreds of parameter combinations were tested, and four of the best combinations were selected based on the criterion of achieving a rate lower than 3 MHz while maximizing the count of physics hits categorized as Local Coincidence.

Finally, the results using these four combinations were compared. The study focused on the impact of energy and the differences between neutrino types. A visualization was employed to demonstrate that only a few physics hits were lost for each neutrino event. Additionally, a new measure called the Minimum Hit Fraction Efficiency was defined, allowing for a clearer comparison of the four proposed sets of parameters. Both efficiencies increased with energy and showed no variation with neutrino type.

In conclusion, two different parameterizations of the pre-trigger LC condition achieved very high efficiencies. Nearly all physics hits were classified as Local Coincidence, with the few that were lost being isolated cases. These lost physics hits were already considered difficult to distinguish from noise from the outset. Therefore, these two potential pre-triggers can be implemented in the IceCube Upgrade planned for 2026.

# Appendices

## A Detailed efficiencies for electron neutrinos

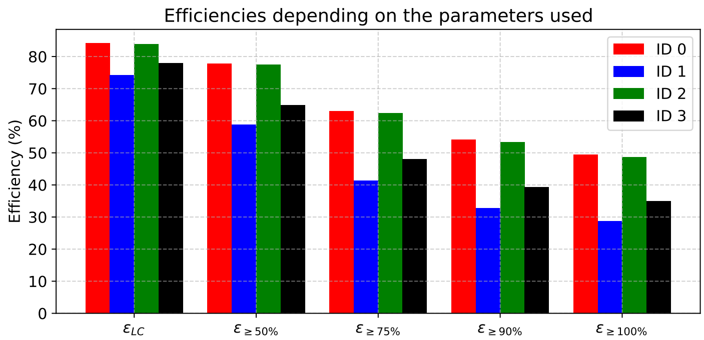


Figure A.1: Efficiencies at low energy 1GeV $\leq$ E $\leq$ 10Gev.

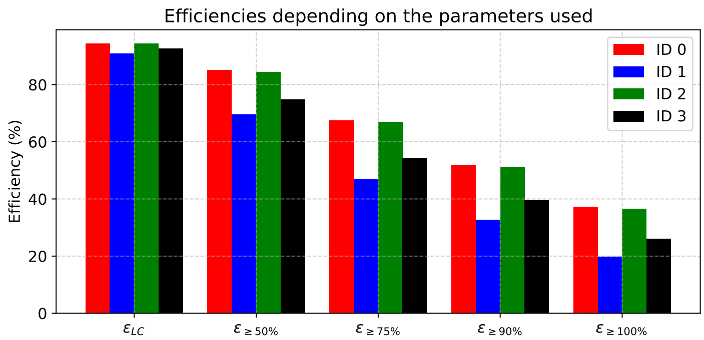


Figure A.2: Efficiencies at mid energy 10GeV $<$ E $\leq$ 100Gev.

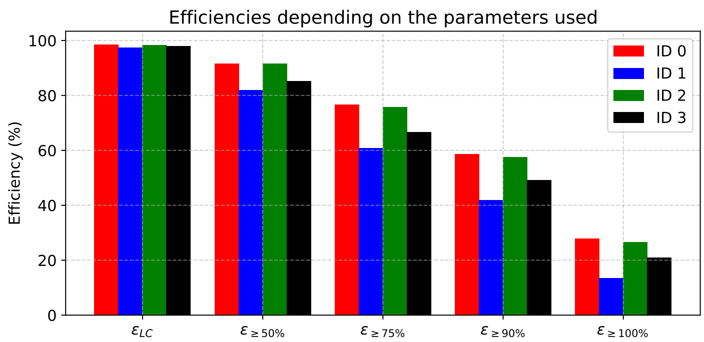


Figure A.3: Efficiencies at high energy 100GeV $<$ E.

# B Minimum Hits Fraction Efficiencies

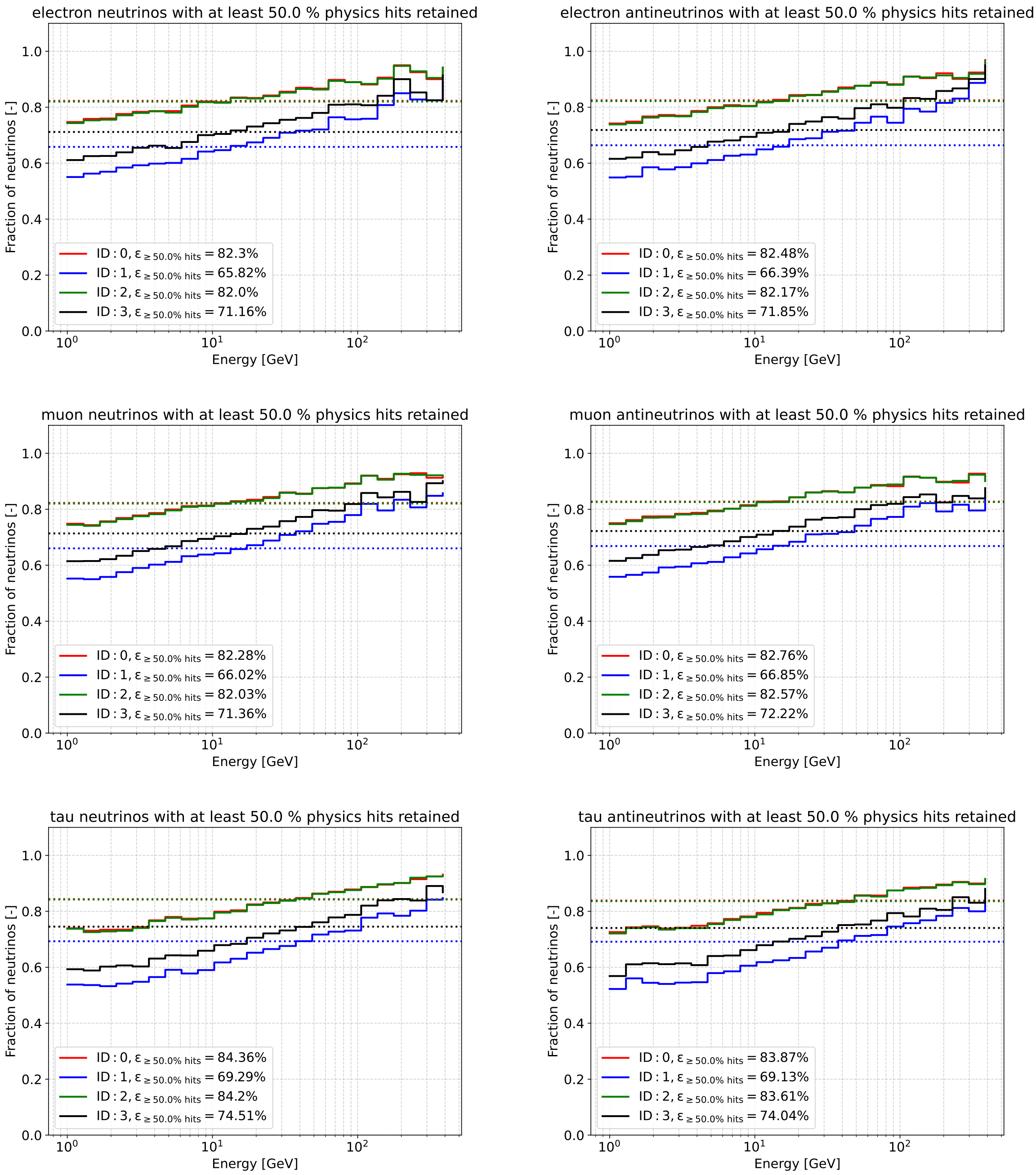


Figure B.1: Minimum Hit Fraction Efficiency at 50%.

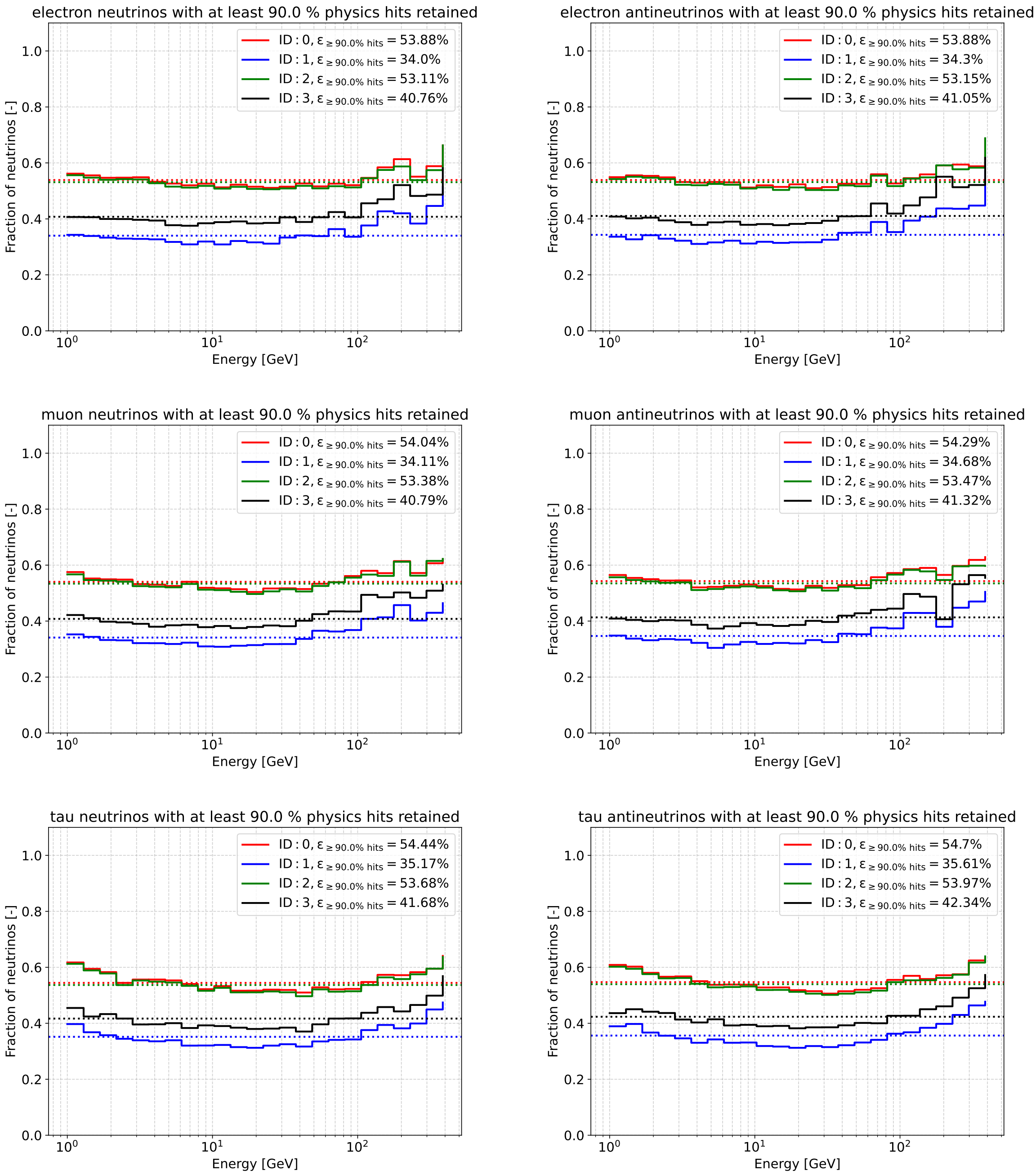


Figure B.2: Minimum Hit Fraction Efficiency at 90%.

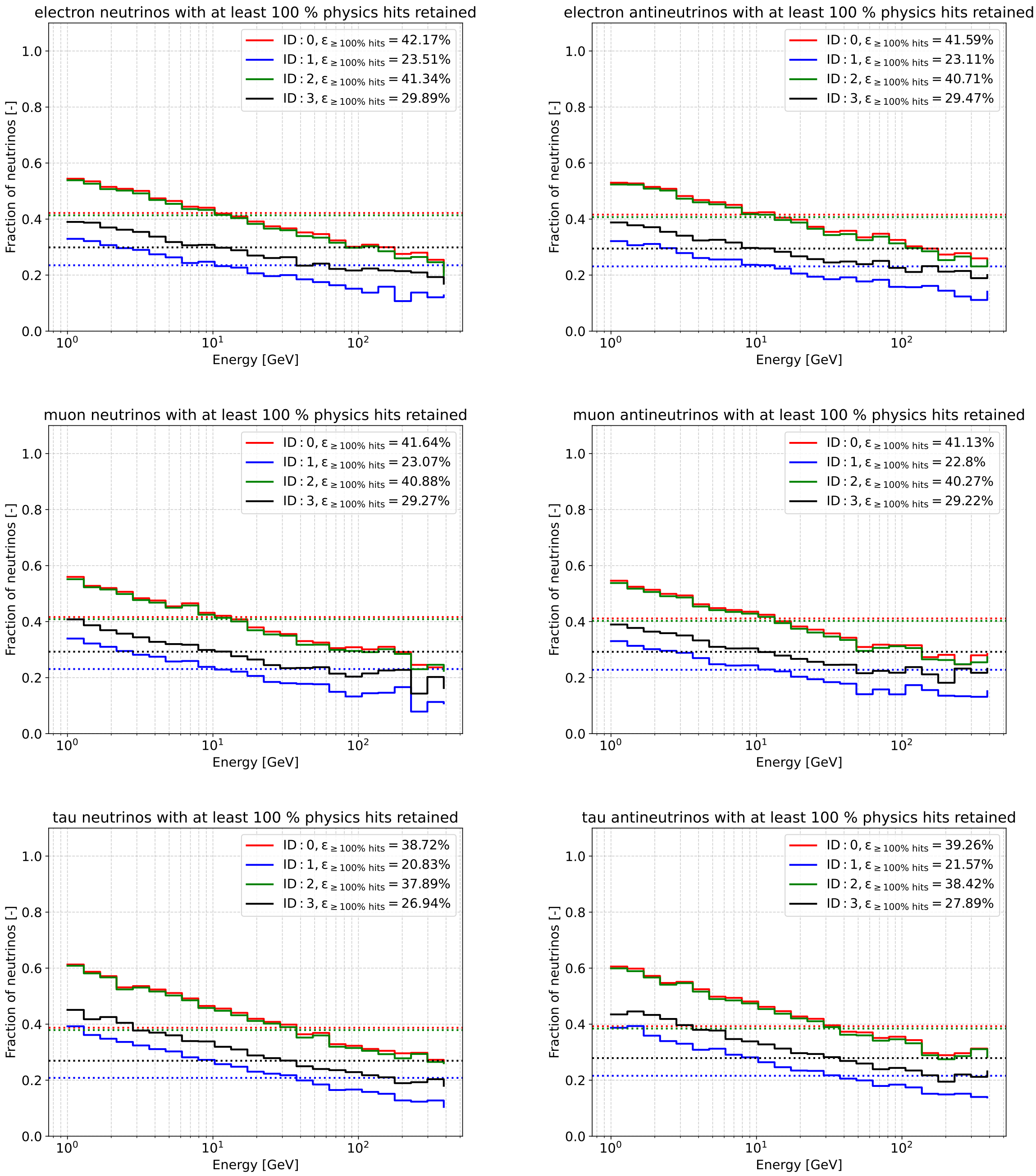


Figure B.3: Minimum Hit Fraction Efficiency at 100%.

# Bibliography

(2025). Icecube. `https://icecube.wisc.edu/science/icecube/`. Accessed: 24/04/2025.

Aartsen, M. (2018). Multimessenger observations of a flaring blazar coincident with high-energy neutrino icecube-170922a. *Science*, 361(6398).

Aartsen, M. et al. (2017). The icecube neutrino observatory: instrumentation and online systems. *Journal of Instrumentation*, 12(03):P03012.

Aartsen, M. G. et al. (2014). Letter of Intent: The Precision IceCube Next Generation Upgrade (PINGU).

Aartsen, M. G. et al. (2015). A combined maximum-likelihood analysis of the high-energy astrophysical neutrino flux measured with icecube. *The Astrophysical Journal*, 809(1):98.

Aartsen, M. G. et al. (2021). Icecube-gen2: the window to the extreme universe. *Journal of Physics G: Nuclear and Particle Physics*, 48(6):060501.

Abbasi, R. et al. (2009). The icecube data acquisition system: Signal capture, digitization, and timestamping. *Nuclear Instruments and Methods in Physics Research Section A: Accelerators, Spectrometers, Detectors and Associated Equipment*, 601(3):294–316.

Abbasi, R. et al. (2021). Design and performance of the multi-PMT optical module for IceCube Upgrade. *PoS*, ICRC2021:1070.

Abbasi, R. et al. (2023a). D-egg: a dual pmt optical module for icecube. *Journal of Instrumentation*, 18(04):P04014.

Abbasi, R. et al. (2023b). Observation of high-energy neutrinos from the galactic plane. *Science*, 380(6652):1338–1343.

Abbasi, R. et al. (2024). Observation of seven astrophysical tau neutrino candidates with icecube. *Physical Review Letters*, 132(15).

Aiello, S. et al. (2025). Observation of an ultra-high-energy cosmic neutrino with KM3NeT. *Nature*, 638(8050):376–382. [Erratum: Nature 640, E3 (2025)].

Andreopoulos, C. et al. (2010). The GENIE Neutrino Monte Carlo Generator. *Nucl. Instrum. Meth. A*, 614:87–104.

Balantekin, A. and Haxton, W. (2013). Neutrino oscillations. *Progress in Particle and Nuclear Physics*, 71:150–161.

Cleveland, B. T., Daily, T., Davis, Jr., R., Distel, J. R., Lande, K., Lee, C. K., Wildenhain, P. S., and Ullman, J. (1998). Measurement of the solar electron neutrino flux with the homestake chlorine detector. *The Astrophysical Journal*, 496(1):505.

Cowan, C. L., Reines, F., Harrison, F. B., Kruse, H. W., and McGuire, A. D. (1956). Detection of the free neutrino: a confirmation. *Science*, 124(3212):103–104.

Danby, G., Gaillard, J.-M., Goulianos, K., Lederman, L. M., Mistry, N., Schwartz, M., and Steinberger, J. (1962). Observation of high-energy neutrino reactions and the existence of two kinds of neutrinos. *Phys. Rev. Lett.*, 9:36–44.

Fargion, D., Oliva, P., and Ucci, G. (2016). Why not any tau double bang in icecube, yet?

Fukuda, Y. et al. (1998). Evidence for oscillation of atmospheric neutrinos. *Physical Review Letters*, 81(8):1562–1567.

Gluesenkamp, T. (2010). *On the Detection of Subrelativistic Magnetic Monopoles with the IceCube Neutrino Observatory*. PhD thesis.

Haxton, W., Hamish Robertson, R., and Serenelli, A. M. (2013). Solar neutrinos: Status and prospects. *Annual Review of Astronomy and Astrophysics*, 51(1):21–61.

Hirata, K. et al. (1987). Observation of a neutrino burst from the supernova sn1987a. *Phys. Rev. Lett.*, 58:1490–1493.

IceCube (2013). Evidence for high-energy extraterrestrial neutrinos at the icecube detector. *Science*, 342(6161).

Kodama, K. et al. (2001). Observation of tau neutrino interactions. *Physics Letters B*, 504(3):218–224.

Kowalski, M. (2017). Neutrino astronomy with icecube and beyond. *Journal of Physics: Conference Series*, 888:012007.

Ma, W. Y. (2020). Physics potential of the icecube upgrade. *Journal of Physics: Conference Series*, 1468:012169.

Mészáros, P. (2017). Astrophysical sources of high-energy neutrinos in the icecube era. *Annual Review of Nuclear and Particle Science*, 67(1):45–67.

Nagai, R. and Ishihara, A. (2019). Electronics development for the new photo-detectors (pdom and d-egg) for icecube-upgrade.

Perl, M. L. et al. (1975). Evidence for anomalous lepton production in $e^+ - e^-$ annihilation. *Phys. Rev. Lett.*, 35:1489–1492.

Reines, F., Crouch, M. F., Jenkins, T. L., Kropp, W. R., Gurr, H. S., Smith, G. R., Sellschop, J. P. F., and Meyer, B. (1965). Evidence for high-energy cosmic-ray neutrino interactions. *Phys. Rev. Lett.*, 15:429–433.

Schwanekamp, H. et al. (2022). Accelerating icecube's photon propagation code with cuda. *Computing and Software for Big Science*, 6.

Spiering, C. (2020). *Neutrino Detectors Under Water and Ice*, pages 785–822. Springer International Publishing, Cham.

Stuerwald, T. (2024). The faint particle trigger for the icecube neutrino observatory.

Yuan, T. (2023). Detecting neutrinos in icecube with cherenkov light in the south pole ice. *Nuclear Instruments and Methods in Physics Research Section A: Accelerators, Spectrometers, Detectors and Associated Equipment*, 1054:168440.

**UNIVERSITE CATHOLIQUE DE LOUVAIN**

**Faculté des sciences**

Place des sciences, 2 bte L6.06.01, 1348 Louvain-la-Neuve, Belgique | **www.uclouvain.be/sc**